

1           **Assessing the biogeography of marine giant viruses in four oceanic transects**

2  
3           Anh D. Ha<sup>1</sup>, Mohammad Moniruzzaman<sup>2</sup>, Frank O. Aylward<sup>1,3\*</sup>

4           <sup>1</sup> Department of Biological Sciences, Virginia Tech, Blacksburg VA, 24061

5           <sup>2</sup> Rosenstiel School of Marine Atmospheric, and Earth Science, University of Miami, Coral  
6           Gables FL 33149

7           <sup>3</sup> Center for Emerging, Zoonotic, and Arthropod-Borne Infectious Disease, Virginia Tech,  
8           Blacksburg VA, 24061

9  
10  
11   **\*Correspondence:**

12   Frank O. Aylward

13   faylward@vt.edu

14  
15   Running title: Biogeography of giant viruses in oceanic transects

16   Keywords: Giant Viruses, Nucleocytoviricota, Mesomimiviridae, Prasinoviridae, marine viruses.

17  
18   **Abstract**

19   Viruses of the phylum *Nucleocytoviricota* are ubiquitous in ocean waters and play important  
20   roles in shaping the dynamics of marine ecosystems. In this study, we leveraged the  
21   bioGEOTRACES metagenomic dataset collected across the Atlantic and Pacific Oceans to  
22   investigate the biogeography of these viruses in marine environments. We identified 330 viral  
23   genomes, including 212 in the order *Imitervirales* and 54 in the order *Algavirales*. We found that  
24   most viruses appeared to be prevalent in shallow waters (<150 meters), and that viruses of the  
25   *Mesomimiviridae* (*Imitervirales*) and *Prasinoviridae* (*Algavirales*) are by far the most abundant  
26   and diverse groups in our survey. Five mesomimiviruses and one prasinovirus are particularly  
27   widespread in oligotrophic waters; annotation of these genomes revealed common stress  
28   response systems, photosynthesis-associated genes, and oxidative stress modulation that may  
29   be key to their broad distribution in the pelagic ocean. We identified a latitudinal pattern in viral  
30   diversity in one cruise that traversed the North and South Atlantic Ocean, with viral diversity

31 peaking at high latitudes of the northern hemisphere. Community analyses revealed three  
32 distinct *Nucleocytoviricota* communities across latitudes, categorized by latitudinal distance  
33 towards the equator. Our results contribute to the understanding of the biogeography of these  
34 viruses in marine systems.

35

## 36 **Introduction**

37 Large DNA viruses of the phylum *Nucleocytoviricota*, also known as “giant viruses”, are a  
38 diverse group of eukaryotic viruses with particle sizes typically larger than 0.2  $\mu\text{m}$  in diameter  
39 and genome sizes reaching up to 2.5 Mbp [1–4]. Known members of the phylum are partitioned  
40 into six orders, namely *Algalvirales*, *Imitevirales*, *Pimascovirales*, *Pandoravirales*, *Asfuvirales*,  
41 and *Chitovirales*, and up to 32 potential families [5]. These viruses have an ancient origin and  
42 have undergone frequent gene exchange with their hosts [6, 7], and as a result their genomes  
43 often encode numerous genes involved in cellular processes such as glycolysis, the TCA cycle,  
44 amino acid metabolism, translation, light sensing, and cytoskeletal dynamics [8–15]. Giant  
45 viruses are known to infect a broad spectrum of eukaryotic hosts; while members of the  
46 *Imitevirales*, *Algalvirales*, and *Pandoravirales* infect a wide range of algae and various  
47 heterotrophic protists, members of the *Asfuvirales*, *Chitovirales*, and *Pimascovirales* infect a  
48 wide range of protist and metazoan hosts [2, 16–19]. The diverse functional repertoires  
49 harbored in these viruses’ genomes are thought to render them able to manipulate the  
50 physiology and subvert the immune responses of their hosts during infection [9, 20, 21]. Giant  
51 viruses therefore play important roles in various ecological processes across the globe.

52 Although giant viruses are ubiquitous in the biosphere, they appear to be particularly abundant  
53 and diverse in marine environments. Early studies focusing on amplification and sequencing of  
54 the viral Family B DNA polymerase from seawater found that algal viruses within the

55 *Nucleocytoviricota* were widespread in a variety of marine environments [22, 23], an observation  
56 which was later confirmed through analysis of community metagenomic data [24, 25]. A recent  
57 comparative metagenomic study found that giant viruses are ubiquitous in the ocean, vary  
58 markedly across depth, and are prevalent in >0.22  $\mu\text{m}$  size fractions [26]. Field studies have  
59 estimated that the abundance of giant viruses can reach up to  $10^4$  -  $10^6$  viruses per milliliter of  
60 seawater, with higher abundances typically recovered during algal blooms [27–32]. Giant  
61 viruses have been reported to infect many prevalent marine eukaryotic lineages, including  
62 chlorophytes, haptophytes, and choanoflagellates [15, 18, 33, 34], and they are therefore an  
63 important factor shaping marine ecological dynamics. Moreover, several studies have shown  
64 that giant viruses associated with algal blooms play key roles in carbon export to deeper waters  
65 [35–37], indicating they are critical components of global carbon cycles. Despite the ecological  
66 importance of giant viruses, our understanding of their diversity lags behind that of smaller  
67 viruses owing to the widespread use of filtration steps in viral diversity surveys, which often  
68 exclude larger viruses [38]. There is therefore a strong need for further studies to examine the  
69 biogeography and ecological dynamics of these large viruses in the ocean.

70 Here, we aimed to undertake a genome-based global survey of giant virus assemblages across  
71 the oceans and compare the diversity of these viruses in different geographic regions by  
72 leveraging the large number of metagenome-assembled genomes (MAGs) of these viruses that  
73 have been generated [9, 39–41]. We focused on the metagenomic data generated from  
74 samples collected in four transects in the Atlantic and Pacific oceans as part of the the  
75 GEOTRACES project [42], which provide clear, well-defined geographic and depth profiles.  
76 These metagenomes targeted the >0.2  $\mu\text{m}$  size fraction and are therefore suitable for examining  
77 the diversity of large viruses. Our work broadens our understanding of the biogeography of giant  
78 viruses in the ocean and reveals novel diversity patterns that will be important for understanding  
79 their role in marine environments.

80

## 81 **Results and Discussion**

82 *Imitervirales* and *Algavirales* orders are the most abundant and diverse among viruses  
83 recovered in bioGEOTRACES metagenomic data set

84 We examined 480 metagenomes collected and sequenced as part of the bioGEOTRACES  
85 component of the GEOTRACES project [42]. These samples were derived from four major  
86 cruises from different regions of the South Pacific and Atlantic Oceans (Fig. 1) in 2010-2011.  
87 This dataset targeted the >0.2- $\mu\text{m}$  size fraction of microbial communities and was sampled  
88 along well-defined transects at various depths, making it suitable for assessing the geographic  
89 and depth distribution of marine giant viruses. In total, we identified 330 giant virus genomes  
90 with metagenomic reads mapping. To investigate the taxonomic distribution of the detected  
91 *Nucleocytoviricota* viruses, we constructed a phylogenetic tree of the viruses and 1,188  
92 *Nucleocytoviricota* reference genomes (Fig. S1; see Methods). Out of the 330 genomes  
93 recovered, we were able to place the genomes within the orders *Imitervirales* [n=214],  
94 *Algavirales* [n=54], *Pimascovirales* [n=16], *Pandoravirales* [n=4], and *Asfuvirales* [n=1]. On the  
95 family level, the most well-represented groups were the *Mesomimiviridae* [n=146] and  
96 *Prasinoviridae* [n=42] (Fig. 2). We also identified 41 *Mirusviricota* viruses; although technically  
97 not members of the *Nucleocytoviricota*, these large DNA viruses are prevalent in the ocean and  
98 share many genomic features with giant viruses [41]. Of the 330 genomes identified, only 8  
99 were derived from cultivated viruses, and 322 genomes are metagenome-assembled genomes  
100 (MAGs). Approximately half (159) of the 330 genomes are larger than 300 kbp (Table S1),  
101 underscoring the prevalence of viruses with large genomes throughout the ocean.

102 Of the 330 genomes with reads mapping, 14 viruses, including 8 *Algavirales* and 5 *Imitervirales*  
103 were recovered in all four bioGEOTRACES transects. Meanwhile, 182 viruses were found in

104 only one transect, among which 116 genomes were found exclusively in transect GA02, most of  
105 which were *Imitervirales* (Fig. 3A, Table S1). In term of total giant virus richness, the number of  
106 different genomes found in transect GA02, which traces along the Americas-Atlantic Ocean  
107 coastline (248 genomes total) by far exceeded that in the other three transects, especially  
108 compared to the pelagic transect GP13 where less than one-third of that number (71 genomes)  
109 were detected. This is likely a consequence of the much broader range of latitudes and  
110 biogeochemical regimes sampled by the GA02 transect compared to the others. Across the  
111 transects, 65 viruses were present in all three depth layers of the water columns (<80m, 80-  
112 150m, and >150m), most of which were *Imitervirales* and *Algavirales* (Fig. 3B). We found 103  
113 viruses that solely appeared in the surface water of 80 meters up, while there were only 5  
114 genomes unique to the deep water of below 150 meters.

115 Giant virus communities were mostly dominated by members of the *Imitervirales* and  
116 *Algavirales* orders, regardless of the transect location or depth of sampling (Fig. 4). On average,  
117 *Imitervirales* and *Algavirales* accounted for 56.4% and 32.6% of the total number of giant virus  
118 occurrences across all sampling locations, respectively. This result is consistent with previous  
119 observations that viruses of these two orders were the most abundant and widespread giant  
120 viruses in the Pacific and Atlantic Ocean [25, 26, 28]. Viruses within the *Imitervirales* were  
121 particularly widespread in communities across all depths sampled in the pelagic GP13 transect,  
122 with a mean contribution of 88.8%, and the majority (9) of the 11 viruses found exclusively in  
123 GP13 were *Imitervirales* (Fig. 2A; Fig. 4C). This pattern of *Imitervirales* dominance in pelagic  
124 waters was also observed in transect GA03 (Fig. 4B, inner samples), underscoring the  
125 prevalence of this group in oligotrophic gyres. In general, the spatial distribution of viruses in the  
126 ocean is shaped largely by the geographic distribution of their hosts [43], and the broad  
127 distribution of viruses within the *Imitervirales* is therefore likely a signature of their collective  
128 broad host range. Indeed, members of the *Imitervirales* order are known to infect an

129 exceptionally broad phylogenetic range of hosts [19], including marine haptophytes in the  
130 genera *Phaeocystis* and *Chrysochromulina*, which were found in high abundance in the open  
131 waters of the central Pacific Ocean [44, 45], as well as other widespread hosts such as the  
132 green algae, Choanoflagellates, and amoeboid protists [15, 46–49]. Aside from these  
133 established hosts, recent work using co-occurrence analyses have also identified a wide range  
134 of other potential eukaryotic hosts for viruses within the *Imitervirales* [12, 50, 51], suggesting  
135 that the hosts of viruses in this order is far broader than currently known. Lastly, given that many  
136 members of the *Imitervirales* gain entry to host cells through phagocytosis, it is likely that  
137 individual viral populations may infect a range of different host lineages. If this is the case, the  
138 broad representation of the *Imitervirales* in pelagic surface waters may represent the ability of  
139 viruses in this order to infect a range of mixotrophic and heterotrophic lineages.

140 The majority of viruses that are most widespread in the Atlantic Ocean in our survey (i.e., found  
141 in all three Atlantic transects GA02, GA03, and GA10, but not in the Pacific transect GP13) were  
142 *Algavirales* viruses (Fig. 3A). Viruses within the *Algavirales* order were especially abundant in  
143 the North Atlantic Ocean (northern samples in transect GA02) and in the coastal waters  
144 (eastern samples in transect GA10) where we observed a high abundance throughout the water  
145 column (Fig. 4A, 4D; Fig. 5C). Viruses of this order were also present in high abundance in  
146 surface waters (<50m) and euphotic waters at 50-150m deep on both two coastal sides of the  
147 transect GA03, while showing a sharp decreasing trend towards the pelagic waters of the North  
148 Atlantic and the Pacific Ocean (inners of transect GA03 and transect GP13, respectively). Once  
149 again, these changes in the abundance of viruses within the *Algavirales* likely reflect the  
150 distribution of their hosts. Members of the family *Prasinoviridae* are the most prevalent family we  
151 identified within the *Algavirales*, and members of this group are known to infect members of the  
152 prasinophyte genera *Ostreococcus*, *Bathycoccus*, and *Micromonas* [18], which have been found  
153 to be highly abundant in coastal systems. It was estimated that prasinophytes may account for

154 50-90% of total picoeukaryotic cells in coastal waters, while they only made up a much lower  
155 fraction (<20%) of those in pelagic waters [52]. Although not as abundant as their counterparts  
156 in coastal populations, there are several prasinophytes found widespread in oligotrophic waters  
157 of the open ocean, for instance *O. lucimarinus* and *Micromonas spp.*, allowing the broad  
158 presence of viruses infecting these hosts, which have been detected and documented [53, 54].  
159 Mirusviruses, *Pimascovirales*, *Pandoravirales*, and *Asfuvirales* were present to a lesser degree  
160 in the four transects, with average contributions of 9.1%, 1.5%, 0.3%, and 0.03% of giant virus  
161 occurrence, respectively. Mirusviruses were prevalent across all four transects (Fig. 4),  
162 consistent with findings of a previous investigation using metagenomic read recruitments from  
163 Tara Oceans datasets [41]. These viruses appeared to be more abundant in coastal waters,  
164 which was maintained throughout the water column (transect GA02 and east of transect GA10),  
165 while in pelagic waters their abundance was more limited to sunlit waters at <100m (inners of  
166 transect GA03 and transect GP13, respectively) (Fig. S2A). This pattern is in agreement with  
167 the prediction that Mirusviruses infect a broad planktonic host range that includes many  
168 phototrophs [41]. All of the *Pimascovirales* genomes recovered in our survey were MAGs  
169 derived from marine metagenomes. Although currently little is known about the natural hosts of  
170 this viral group in the oceans, their prevalence across the four transects suggests that they  
171 infect widespread host taxa and play important roles in marine systems. Interestingly, we found  
172 that the recently-delineated family-level clade PM\_01 was the most prevalent lineage of the  
173 *Pimascovirales* in the ocean, but no members of this group have been cultivated and their host  
174 range remains unknown. A recent study found a member of this lineage was prevalent in  
175 surface waters of Station ALOHA, consistent with the view that they are present in oligotrophic  
176 surface waters [55]. The only *Asfuvirales* virus found in our survey, GVMAG-M-3300027833-19  
177 was recovered in the GA10 transect, which is located off the Atlantic coast of South Africa. This  
178 viral genome was also recently recovered in a TARA metagenomic sample in the same region

179 [17] and its transcriptomic activities were detected in the waters of the central California Current  
180 upwelling system in the North Pacific Ocean [12], suggesting that the virus may be widely  
181 distributed beyond the sampling scope of the bioGEO TRACES cruises. *Pandoravirales* viruses  
182 were present in all four transects in both coastal and pelagic waters, although at relatively low  
183 number of occurrences and abundance. Across all locations included in our survey, their  
184 distribution was strictly limited to shallower waters (<150 meters) (Fig. S2C). The  
185 *Pandoravirales* includes well-studied coccolithoviruses that are prevalent in *Emiliania huxleyi*  
186 blooms, suggesting that at least some members of this order will have highly variable  
187 abundance depending on host availability. An important caveat of our study is that we surveyed  
188 only metagenomes derived from >0.2  $\mu\text{m}$  size fractions; it is likely that some members of the  
189 *Pimascovirales* and *Asfuvirales*, which have on average smaller genome and virion sizes than  
190 members of the *Imitervirales*, may be more widespread in smaller size fractions, and are  
191 therefore more prevalent than indicated by our results here.

192 Giant viruses were apparently more diverse and abundant in surface waters (Fig. 3B, Fig. 4).  
193 Indeed, of all occurrences of giant viruses throughout the water column at all locations, 92.1%  
194 were located in waters at 150 meters or shallower. On average across all four transects, the  
195 viral richness at two depth ranges (<80m and 80-150m) were approximately 2.7 and 2.3 times  
196 higher than that at deep waters ( $\geq 150\text{m}$ ), respectively (Kruskal–Wallis and Dunn’s test,  
197  $P < 0.001$ ) (Fig. S3). In transects GA03 and GP13, the decline in total giant virus abundance with  
198 depth was particularly sharp (Fig. 5A). In deeper pelagic water (>200m), the giant communities  
199 appeared to be limited to just a few members of the *Imitervirales* (inners of transect GA03 and  
200 transect GP13), while in coastal waters at deeper than 200m, members of the *Algavirales* are  
201 also present with relatively high abundance, together with *Imitervirales* viruses (Fig. 4, Fig. 5).  
202 Apart from viruses of the *Algavirales* and *Imitervirales* orders, our read mapping approach did  
203 not recover any giant virus MAGs of any other orders in metagenomes sequenced from water

204 sampled from depths >200m. This may be partially due to biases in the reference database,  
205 which includes more genomes from surface water samples, but it seems likely that it is at least  
206 partially driven by the large diversity of giant viruses in surface waters.

207

### 208 *Latitudinal pattern of giant virus diversity*

209 We analyzed the giant virus communities along the transect GA02 in more detail to assess  
210 possible latitudinal gradients in giant virus diversity. The GA02 transect sampling sites follows  
211 the Americas-Atlantic Ocean coastline, spanning across a long range of latitudes from the  
212 parallel 50° North to 50° South and tracing a clear latitudinal gradient from the North Atlantic in  
213 the summer of 2010 to the south Atlantic in the austral summer of 2011. This sampling scheme  
214 may facilitate the detection of subtle latitudinal gradients that may be more difficult to resolve  
215 through comparison of samples collected across different ocean basins. In terms of community  
216 composition at each sampling location, the *Algavirales* assemblages seemingly dominated the  
217 giant virus communities in northern samples and decreased in abundance towards the south,  
218 replaced by the dominance of viruses of the order *Imitervirales* (Fig. S4).

219 We calculated taxonomic richness and Shannon's H diversity index in each depth-integrated  
220 sampling location to investigate latitudinal variation (Fig. 6). To avoid biases in diversity  
221 measurements due to unequal sequencing depth, we rarefied all metagenomic samples to 10M  
222 reads prior to calculation. We detected a latitudinal pattern of diversity along the GA02 transect  
223 with average diversity increasing with higher latitudes in the Northern Hemisphere and  
224 plateaued towards the South. Total giant virus communities peaked, both in terms of richness  
225 and alpha diversity in the further north of the North Atlantic Ocean (i.e. above 40° North) and  
226 steeply declined around the middle latitudes (20-40° North). The trend of increasing diversity  
227 from the equatorial zone towards higher latitudes was mirrored in the *Imitervirales* communities,

228 while varying marginally in the *Algavirales* communities for both viral genome richness and  
229 alpha diversity (Fig. 6). The clear peak in latitudinal diversity in the Northern Hemisphere is  
230 consistent with the trend of species richness observed for a large portion of the total of 65,000  
231 marine species examined previously [56]. It is possible that stronger environmental instability,  
232 particularly the wide temperature variation in the northern hemisphere (excluding polar zones)  
233 [57] may explain the higher diversity compared to the south. A relatively similar northern spike of  
234 giant virus diversity has been reported from analyses of the Family B DNA Polymerase (PolB)  
235 genes in Tara Oceans datasets [26, 58], although the studies observed another increase in  
236 diversity near the southern middle latitudes. The discrepancy did not seem to result from the  
237 disparity in methodological approaches between our mapping strategy and the above two  
238 studies; we also performed calculation of diversity indices on the TARA Ocean datasets using  
239 our mapping method described herein, and observed a similar trend in giant virus diversity  
240 agreeing with in the two PolB studies in latitudinal locations of elevated diversity (Fig. S5). It is  
241 possible that the slightly differing results reflects the fact that the bioGEOTRACES and Tara  
242 Oceans samples were collected from different times with different cruise tracks.

243 The lower diversity, in terms of alpha diversity and richness of the giant virus communities near  
244 the equator in comparison with northern high latitudes did not follow conventional latitude  
245 diversity pattern, which posits that marine eukaryotic diversity generally increases toward the  
246 tropics [58, 59]. The difference could possibly be attributed to several potential causes. High  
247 temperature in the equatorial zone is potentially one underlying cause; decline in species  
248 diversity at higher temperatures has been observed in several marine taxa [60]. Previous work  
249 has widely reported that marine species tend to shift away from the tropics to higher latitudes  
250 due to climate warming [61–63]. A species distribution model has projected that marine species  
251 may acquire latitudinal peaks in total richness at approximately 40/30° absolute latitude and a  
252 loss of richness near the equator, highlighting the important role of temperature on these

253 distribution shifts [64]. Indeed, the metagenomic samples located in the GA02 transect included  
254 in our survey were collected during the months from late March to June, which were anticipated  
255 to be the warmest months of the year in the equatorial Atlantic Ocean [65]. Given the strong  
256 influence of seasonality on marine microbial communities, it is likely that latitudinal gradients in  
257 diversity are ephemeral and will vary throughout the year.

258 A non-metric multidimensional scaling (NMDS) analysis indicated that *Nucleocytoviricota*  
259 communities were clustered according to their latitudinal distance to the equator (Fig. 7). The  
260 giant virus community composition significantly differed between three latitudinal sectors in both  
261 the GA02 transect exclusively and all transects collectively (Permanova  $p < 0.001$ ). This  
262 clustering is fairly consistent with traditional Longhurst oceanographic biogeographical biomes  
263 of plankton ecology, which were designated based on the distribution of chlorophyll, angle of  
264 sunlight, and cloudiness [66]. This may further support the view that the geographic distribution  
265 of viruses in ocean waters is mostly affected by the distribution of their hosts. In terms of viral  
266 community richness, we found only 5 giant virus genomes (2% of the total number of giant  
267 viruses found in the GA02 transect) shared across all three latitudinal zones (Fig. S6), all of  
268 which belonged to the order *Algavirales*. The high latitude zone ( $>40^\circ$  latitude) harbored 93  
269 unique genomes, while the mid-latitude zone ( $20^\circ$  to  $40^\circ$  latitude) had 68 and the low latitude  
270 zone (between  $20^\circ$  equatorial) had 24.

271

272 *Five Mesomimiviruses and one prasinovirus are particularly widespread in oligotrophic waters*

273 The vast majority of the most abundant and widespread viruses in our survey belong to the  
274 orders *Imitervirales* and *Algavirales*. We observed six MAGs within the *Imitervirales* (5  
275 genomes) and the *Algavirales* (1 genome) that were particularly widespread in oligotrophic  
276 waters (Fig. 8A), all detected across different water depths in at least 19 distinct sampling

277 locations. All the five *Imitervirales* could be classified into the recently-proposed  
278 *Mesomimiviridae* family (*Imitervirales* family 1) (Table S1). The *Mesomimiviridae* family is  
279 particularly widespread in marine systems and contains well-documented cultivated  
280 representatives that infect oceanic haptophytes, such as *Phaeocystis globosa* virus (PgV),  
281 *Chrysochromulina ericina* virus (CeV), and *Chrysochromulina parva* virus (CpV) [67–69]. Other  
282 members of the family have been found co-occurring and correlating with diatoms [50],  
283 suggesting that diatoms are potential hosts of this viral lineage. The only *Algavirales* virus  
284 belonged to the *Prasinoviridae* family (*Algavirales* family 1). The most broadly distributed  
285 genome, ERX556088.18.dc was recovered in 122 samples (more than 25% of the total number  
286 of samples analyzed overall) at 34 sampling locations. All the five Mesomimiviruses were  
287 extensively distributed in the Pacific transect GP13, while the prasinovirus,  
288 TARA\_IOS\_NCLDV\_00011, was more widespread in the Atlantic Ocean (Fig. S7). All of these  
289 six genomes derived from marine environments, with genome sizes ranging from 108,412 bp to  
290 483,524 bp and GC content varied from 26.2% to 34.6%.

291 Annotation of these genomes showed complex genomic repertoires, which is a common  
292 characteristic of viruses of the *Mesomimiviridae* and the *Prasinoviridae*. Complete or near-  
293 complete set of 9 giant virus core genes, including major capsid protein (MCP), A32-like  
294 packaging ATPase (A32), superfamily II helicase (SFII), family B DNA Polymerase (PolB), virus  
295 late transcription factor 3 (VLTf3), large and small RNA polymerase subunits (RNAPL and  
296 RNAPS, respectively), TFIIB transcriptional factor (TFIIB), and Topoisomerase family II (TopoII)  
297 were found in all of the *Mesomimiviridae* genomes, indicating that these are high quality  
298 genome assemblies (Fig. 8B). These core genes are broadly represented in genomes of  
299 *Nucleocytoviricota* and have previously been used as phylogenetic markers for these viruses [5,  
300 7, 70]. Both RNAP subunits were absent in the *Prasinoviridae* genome, consistent with the lack  
301 of DNA-dependent RNA polymerase that has been previously reported for prasinoviruses [11].

302 Other genes encoding essential viral functions were also consistently found in these genomes,  
303 including ribonucleotide reductase, thymidylate synthase, dUTPase (for nucleotide metabolism),  
304 Nudix-like hydrolase, mRNA capping enzyme (transcription and RNA processing), and  
305 glycosyltransferase (virion morphogenesis) (Table S2).

306 Genes involved in translation have been widely reported in the genomes of viruses within the  
307 order *Imitervirales* [71–73]. We found several translation-related genes, including aminoacyl-  
308 tRNA synthetases, or aaRS (asparaginyl-tRNA synthetase), translation initiation factors (IF4E,  
309 eIF3, IF1A), translation elongation factors (eF-TU) in all of the *Mesomimiviridae* genomes. The  
310 aaRS genes catalyzes the linkage between tRNAs and amino acids during translation and may  
311 act as a mechanism for circumventing nutrient starvation in the host cell, allowing the virus to  
312 maintain viral replication in different nutritional conditions [74].

313 Throughout all six genomes, we also identified numerous genes involved in diverse metabolic  
314 processes (Fig. 8B, Table S2), which may be involved in rewiring host metabolism and cellular  
315 physiology during infection to support their own viral production. We found genes involved in  
316 central carbon metabolism, including enzymes for glycolysis, the TCA cycle, and beta oxidation  
317 in all of the genomes. Numerous genes involved in nutrient acquisition and processing, light-  
318 driven energy generation, and diverse transporters were also present, consistent with previous  
319 findings [9, 39]. Rhodopsins could potentially alter the host's sunlight-dependent energy transfer  
320 system [15], while chlorophyll a/b binding proteins might help maintain a stable light-harvesting  
321 capacity of host cells during infection [9]. The presence of genes involved in photosynthetic  
322 processes might be important for these viruses to infect a wide array of phototrophic or  
323 mixotrophic hosts in well-lit waters across the ocean. Genes encoding storage proteins and  
324 transporters, including ferritin-like proteins, amino acid permeases, transporters predicted to  
325 target sulfur, phosphorus, and iron are common in these genomes and may have a role in  
326 rewiring host's nutrient acquisition strategies to enhance viral propagation. Such set of viral-

327 encoded nutrient storage and transporters might be especially advantageous in marine  
328 environments, particularly in the oligotrophic waters of the South Pacific Ocean, where  
329 micronutrients such as iron are scarce [75] and the viruses need to employ their own  
330 transporters to boost nutrient acquisition. We also found homologs of genes involved in the  
331 regulation of cellular apoptosis, including caspase and tumor necrosis factor receptor.  
332 Manipulation of cell death is a common strategy employed by giant viruses to avert the  
333 impending cellular response to viral infection [76–78].

334 A broad array of stress response and repair genes found in all of the six genomes potentially  
335 equips the viruses with the ability to endure various external stresses common in oligotrophic  
336 waters, such as high temperatures, ultraviolet (UV) damage, and oxidative stress. We found  
337 genes involved in oxidative stress regulation, including thioredoxin, glutaredoxin, and  
338 superoxide dismutase (SOD) to be common among all genomes. Thioredoxin and SOD have  
339 been found expressed in several members of the *Imitervirales* [9, 79, 80] and were suggested to  
340 mitigate cellular oxidative stress by detoxifying harmful reactive oxygen species released by  
341 hosts during viral infection. SOD may also play an active role in reducing superoxide  
342 accumulation induced by UV exposures in direct sunlight, which may aid survival of viruses in  
343 the sunlit open waters [81]. It has been postulated that such viral-encoded redox genes allow  
344 the virus to infect a broad range of hosts [80]. Previous work has noted that giant viruses may  
345 carry genes that serve their own DNA repair to maintain high fidelity in genome replication [70,  
346 82, 83]. We identified various DNA repair genes, including MutS mismatch repair and ultraviolet  
347 (UV) damage repair, such as ERCC4 nuclease [84] to be present in all of the mesomimivirus  
348 genomes. MutS homologs are widely present in genomes of mimivirus relatives [67, 85, 86] and  
349 are thought to associate with correcting mismatches to ensure the fidelity of viral genome  
350 replication. ERCC4-type repair nuclease might provide the viruses with crucial protection  
351 against DNA damages caused by UV irradiation. Although the prasinovirus' genome lack

352 homologs of MutS and ERCC4-type repair nuclease, it encodes numerous other putative DNA  
353 repair genes such as phosphatidylinositol 3-kinase and PD-(D/E)XK nuclease superfamily,  
354 which could also potentially aid in maintaining DNA integrity.

355 We also identified various genes predicted to encode enzymes for synthesizing glycans, which  
356 may be involved in the decoration of capsids with sugar moieties. These viral-encoded fibril  
357 structures are potentially useful for viruses to extend their host range and persist in the open  
358 waters. First, the oligosaccharides may enable the modification of virion surface to mimic the  
359 host's normal food source, e.g. organic debris and bacteria [87, 88], promoting phagocytosis of  
360 virion particles. This strategy of infection, which takes advantage of the 'generalized' feeding  
361 habit that many marine protists rely on, may obviate the requirement of building receptors to a  
362 specific host and thus allow for a broader array of hosts. In addition, glycosylated fibrils could  
363 possibly act as a protective layer to shield the viruses from unfavorable environmental  
364 conditions, therefore increasing viral persistence. Furthermore, a study of *Acanthamoeba*  
365 polyphaga mimivirus has found that viral particles covered with self-produced sugars are able to  
366 adhere to different organisms through glycoside interactions, including bacteria, fungi, and  
367 arthropods [89], without infecting them. These organisms thus may help disperse the viruses  
368 over a wide area of waters, increasing their chance of contact with drifted host cells and  
369 expanding spatial distribution across the ocean. We also observed that all of these viruses carry  
370 lectin-domain containing proteins, which may act as key mediators of host-virus recognitions  
371 and interactions [90, 91]. Although the exact role of the protein in viruses is still unclear, it is  
372 possible that they might leverage lectin domains to modulate interactions with hosts and  
373 achieve a broader host range.

374

375 **Conclusion**

376 In this study we conducted a metagenomic survey of giant viruses in the Atlantic and Pacific  
377 Oceans using the bioGEOTRACES datasets. We show that giant viruses of the orders  
378 *Imitervirales* and *Algavirales* are particularly widespread and abundant in epipelagic waters.  
379 Giant virus communities vary markedly by latitude, and in the GA02 transect in the Atlantic  
380 Ocean we detected a latitudinal pattern of diversity that peaks at high northern latitudes and  
381 plateaus towards the south. Lastly, we identified five genomes of the *Mesomimiviridae* family of  
382 the *Imitervirales* and one genome of the *Prasinoviridae* of the *Algavirales* that are particularly  
383 widespread in oligotrophic waters. Our comparative genomic analysis revealed that these  
384 genomes encoded diverse genes involved in central carbon metabolism, stress responses, and  
385 lectin-domain proteins potentially involved in host-virus interactions. We hypothesize that these  
386 genes may collectively expand the host range of these viruses, possibly explaining their  
387 particularly broad distribution. Overall, our study provides genomic insights into the distribution  
388 of giant viruses in the ocean and sheds light on the biogeography of these ecologically-  
389 important community members.

390

## 391 **Materials and Methods**

### 392 *Nucleocytoviricota* genome database compilation

393 We downloaded 1,382 *Nucleocytoviricota* genomes from the Giant Virus Database [5] and 696  
394 viral MAGs assembled from 937 Tara Oceans metagenomes within the Global Ocean  
395 Eukaryotic Viral database [41]. All of these genomes were classified to the phylum  
396 *Nucleocytoviricota*, except those of the recently-discovered *Mirusviricota* lineage, which has a  
397 herpesvirus-like capsid and likely belongs to the realm Duplodnaviria. Although Mirusviruses  
398 represent a lineage distinct from the *Nucleocytoviricota*, we included them here because they  
399 represent a widespread lineage of marine large DNA viruses, and their genomes appear to be a

400 chimera of different viral lineages, including the *Nucleocytoviricota*. To remove possible  
401 contamination from cellular sources, we screened all viral genomes using ViralRecall [92] and  
402 removed all contigs that had a score < 0 (indicating stronger signals from cellular sources). We  
403 also excluded genomes of less than 100 kbp total sequence, not encoding PoIB gene, and/or  
404 containing less than 2 out of 4 of the marker genes SFII, TFIIIB, VLTF3, and A32. To avoid the  
405 presence of identical or highly similar genomes, we dereplicated the genome set with dRep  
406 v3.2.2 [93] using an average nucleotide identity threshold of 95%. We arrived at a database  
407 containing 1,629 viral genomes (1,518 *Nucleoviricota* and 111 *Mirusviricota*) for metagenomic  
408 read mapping.

409

#### 410 *Metagenome data set*

411 We examined the metagenomic data from the >0.2- $\mu$ m size fraction microbial communities of  
412 480 samples collected by the international GEOTRACES program from May 2010 to December  
413 2011. Accession numbers of the data are listed in Table S3. The samples were collected in four  
414 major cruise transects (GA02, GA03, GA10, and GP13) across the Atlantic and Pacific Oceans  
415 at 2-10 depths in each sampling location, ranging from 6m to 5601m. Sample processing was  
416 previously described in detail [42]. We calculated the geographical distance between sample  
417 locations in each transect based on recorded latitudes and longitudes using the function  
418 distHaversine from the R package geosphere.

419

#### 420 *Reads processing and mapping*

421 We downloaded and trimmed reads from each of the metagenome samples with Trim Galore v.  
422 0.6.4 using parameters “-length 50 -e 0.1 -q 5 -stringency 1 --phred33”. We then mapped the  
423 trimmed reads onto the *Nucleocytoviricota* nucleotide sequences using coverM v0.6.1  
424 (<https://github.com/wwood/CoverM>) in mode ‘genome’, with the parameter --min-read-percent-  
425 identity 0.95. We calculated relative abundance in reads mapped per kilobase of genome, per

426 million mapped reads (RPKM). To avoid the false detection of viral genomes due to spurious  
427 read mapping, we only retained genomes with breadth coverage >20% (i.e. more than 20% of  
428 the genome length were covered by any read) in subsequent analyses. This cutoff is based on  
429 recent work which suggested that a genome coverage of at least 20% is appropriate to indicate  
430 the presence of that genome in a sample [94]. After this filtering, we obtained a set of 330  
431 *Nucleocytoviricota* genomes for subsequent analysis.

432

#### 433 *Phylogeny and clade delineation.*

434 To provide phylogenetic context for the giant virus genomes that we identified, we constructed a  
435 multilocus phylogenetic tree of the *Imitervirales* order using a set of 7 marker genes: family B  
436 DNA Polymerase (PolB), A32-like packaging ATPase (A32), Poxvirus late transcription factor 3  
437 (VLTF3), superfamily II helicase (SFII), alpha RNA polymerase subunits (RNAPL), TFIIB  
438 transcriptional factor (TFIIB), and Topoisomerase family II (TopoII). The concatenated alignment  
439 of these 7 markers was generated with the `ncldv_markersearch.py` script  
440 ([github.com/faylward/ncldv\\_markersearch](https://github.com/faylward/ncldv_markersearch)) and then trimmed with TrimAl v. 1.4.rev22 [95]  
441 (parameter `-gt 0.1`). The tree was inferred from the alignment using IQ-TREE version 2.2.0.3  
442 [96] with the best fitting model determined by the ModelFinder Plus option in IQ-TREE,  
443 according to the Bayesian Information Criterion (BIC). We used the same order-, family-, and  
444 genus-level nomenclature for the *Nucleocytoviricota* as previously described [5].

445

#### 446 *Subsampling reads and calculating diversity*

447 Comparison of diversity among samples, especially alpha diversity, may be erroneous due to  
448 differing library sizes [97]. To ensure equal library sizes across samples for diversity  
449 measurements, all samples were randomly subsampled without replacement to 10M reads  
450 using the `reformat` program provided in `bbtools` suite (Bushnell B. –  
451 [sourceforge.net/projects/bbmap/](https://sourceforge.net/projects/bbmap/)). The subsampled reads were mapped against the viral

452 genome set using coverM as described above. We then calculated community richness and  
453 Shannon's diversity indices using the package 'vegan' ([https://cran.r-](https://cran.r-project.org/web/packages/vegan/)  
454 [project.org/web/packages/vegan/](https://cran.r-project.org/web/packages/vegan/)). Variation among community composition was analyzed with  
455 NMDS ordination based on Bray–Curtis dissimilarity using the function 'metaMDS', parameters  
456  $k = 2$ ,  $trymax = 100$ . Statistical analyses of difference in community composition were performed  
457 using a PERMANOVA test with the 'adonis' function, 9,999 permutations.

458

#### 459 *Depth distribution mapping and interpolation*

460 We performed interpolation of viral depth distribution using the program Ocean Data View  
461 v5.6.0 [98] in DIVA gridding mode, with parameters signal-to-noise = 25, automatic scale  
462 lengths for the X- and Y-axis, quality limit = 3 to exclude bad estimates.

463

#### 464 *Protein annotations*

465 We annotated proteins in six widespread giant virus genomes by comparing them to the  
466 EggNOG database 5.0.0 [99] and Pfam-A release 34 [100] hidden Markov models (HMMs)  
467 profile using HMMER v3.3.2 (parameter "-E 1e-3" for the EggNOG search and "-cut\_nc" for the  
468 Pfam search) and retained only the best hits.

469

#### 470 **Data availability**

471 The data sets analyzed in this study are already publicly available and were accessed as  
472 described in the Materials and Methods section.

473

#### 474 **Acknowledgements**

475 We would like to thank the authors of Biller et al for providing access to the GEOTRACES  
476 metagenomes used in this study. We acknowledge the use of the Virginia Tech Advanced  
477 Research Computing Center for bioinformatic analyses performed in this study.

478

#### 479 **Competing interests**

480 The authors declare no competing interests.

481

#### 482 **Funding**

483 National Science Foundation (CAREER-2141862 to F.O.A.); Simons Early Career Award in  
484 Marine Microbial Ecology and Evolution (to F.O.A.), National Institutes of Health  
485 (1R35GM147290-01 to F.O.A).

486

#### 487 **References**

- 488 1. Koonin EV, Dolja VV, Krupovic M, Varsani A, Wolf YI, Yutin N, et al. Global Organization  
489 and Proposed Megataxonomy of the Virus World. *Microbiol Mol Biol Rev* 2020; **84**.
- 490 2. Wilhelm S, Bird J, Bonifer K, Calfee B, Chen T, Coy S, et al. A Student's Guide to Giant  
491 Viruses Infecting Small Eukaryotes: From Acanthamoeba to Zooxanthellae. *Viruses* .  
492 2017. , **9**: 46
- 493 3. Fischer MG. Giant viruses come of age. *Curr Opin Microbiol* 2016; **31**: 50–57.
- 494 4. Aylward FO, Moniruzzaman M. Viral Complexity. *Biomolecules* 2022; **12**.
- 495 5. Aylward FO, Moniruzzaman M, Ha AD, Koonin EV. A phylogenomic framework for charting  
496 the diversity and evolution of giant viruses. *PLoS Biol* 2021; **19**: e3001430.
- 497 6. Moniruzzaman M, Weinheimer AR, Martinez-Gutierrez CA, Aylward FO. Widespread  
498 endogenization of giant viruses shapes genomes of green algae. *Nature* 2020; **588**: 141–

- 499 145.
- 500 7. Guglielmini J, Woo AC, Krupovic M, Forterre P, Gaia M. Diversification of giant and large  
501 eukaryotic dsDNA viruses predated the origin of modern eukaryotes. *Proc Natl Acad Sci U*  
502 *S A* 2019; **116**: 19585–19592.
- 503 8. Blanc-Mathieu R, Dahle H, Hofgaard A, Brandt D, Ban H, Kalinowski J, et al. A persistent  
504 giant algal virus, with a unique morphology, encodes an unprecedented number of genes  
505 involved in energy metabolism. *J Virol* 2021.
- 506 9. Moniruzzaman M, Martinez-Gutierrez CA, Weinheimer AR, Aylward FO. Dynamic genome  
507 evolution and complex virocell metabolism of globally-distributed giant viruses. *Nat*  
508 *Commun* 2020; **11**: 1710.
- 509 10. Rodrigues RAL, Arantes TS, Oliveira GP, Dos Santos Silva LK, Abrahão JS. The Complex  
510 Nature of Tupanviruses. *Adv Virus Res* 2019; **103**: 135–166.
- 511 11. Moreau H, Piganeau G, Desdevises Y, Cooke R, Derelle E, Grimsley N. Marine  
512 prasinovirus genomes show low evolutionary divergence and acquisition of protein  
513 metabolism genes by horizontal gene transfer. *J Virol* 2010; **84**: 12555–12563.
- 514 12. Ha AD, Moniruzzaman M, Aylward FO. High Transcriptional Activity and Diverse Functional  
515 Repertoires of Hundreds of Giant Viruses in a Coastal Marine System. *mSystems* 2021; **6**:  
516 e0029321.
- 517 13. Yutin N, Koonin EV. Proteorhodopsin genes in giant viruses. *Biol Direct* 2012; **7**: 34.
- 518 14. Rozenberg A, Oppermann J, Wietek J, Fernandez Lahore RG, Sandaa R-A, Bratbak G, et  
519 al. Lateral Gene Transfer of Anion-Conducting Channelrhodopsins between Green Algae  
520 and Giant Viruses. *Curr Biol* 2020; **30**: 4910–4920.e5.
- 521 15. Needham DM, Yoshizawa S, Hosaka T, Poirier C, Choi CJ, Hehenberger E, et al. A distinct  
522 lineage of giant viruses brings a rhodopsin photosystem to unicellular marine predators.  
523 *Proceedings of the National Academy of Sciences* . 2019. , **116**: 20574–20583
- 524 16. Koonin EV, Yutin N. Evolution of the Large Nucleocytoplasmic DNA Viruses of Eukaryotes

- 525 and Convergent Origins of Viral Gigantism. *Adv Virus Res* 2019; **103**: 167–202.
- 526 17. Karki S, Moniruzzaman M, Aylward FO. Comparative Genomics and Environmental  
527 Distribution of Large dsDNA Viruses in the Family Asfarviridae. *Frontiers in Microbiology* .  
528 2021. , **12**
- 529 18. Weynberg KD, Allen MJ, Wilson WH. Marine Prasinoviruses and Their Tiny Plankton Hosts:  
530 A Review. *Viruses* 2017; **9**.
- 531 19. Claverie J-M, Abergel C. Mimiviridae: An Expanding Family of Highly Diverse Large dsDNA  
532 Viruses Infecting a Wide Phylogenetic Range of Aquatic Eukaryotes. *Viruses* . 2018. , **10**:  
533 506
- 534 20. Rosenwasser S, Ziv C, van Creveld SG, Vardi A. Virocell Metabolism: Metabolic  
535 Innovations During Host–Virus Interactions in the Ocean. *Trends in Microbiology* . 2016. ,  
536 **24**: 821–832
- 537 21. Forterre P. Manipulation of cellular syntheses and the nature of viruses: The virocell  
538 concept. *C R Chim* 2011; **14**: 392–399.
- 539 22. Chen F, Suttle CA, Short SM. Genetic diversity in marine algal virus communities as  
540 revealed by sequence analysis of DNA polymerase genes. *Appl Environ Microbiol* 1996;  
541 **62**: 2869–2874.
- 542 23. Short SM, Suttle CA. Sequence analysis of marine virus communities reveals that groups of  
543 related algal viruses are widely distributed in nature. *Appl Environ Microbiol* 2002; **68**:  
544 1290–1296.
- 545 24. Monier A, Larsen JB, Sandaa R-A, Bratbak G, Claverie J-M, Ogata H. Marine mimivirus  
546 relatives are probably large algal viruses. *Virology* 2008; **5**: 12.
- 547 25. Monier A, Claverie J-M, Ogata H. Taxonomic distribution of large DNA viruses in the sea.  
548 *Genome Biol* 2008; **9**: R106.
- 549 26. Endo H, Blanc-Mathieu R, Li Y, Salazar G, Henry N, Labadie K, et al. Biogeography of  
550 marine giant viruses reveals their interplay with eukaryotes and ecological functions. *Nat*

- 551 *Ecol Evol* 2020; **4**: 1639–1649.
- 552 27. Bellec L, Grimsley N, Derelle E, Moreau H, Desdevises Y. Abundance, spatial distribution  
553 and genetic diversity of *Ostreococcus tauri* viruses in two different environments. *Environ*  
554 *Microbiol Rep* 2010; **2**: 313–321.
- 555 28. Hingamp P, Grimsley N, Acinas SG, Clerissi C, Subirana L, Poulain J, et al. Exploring  
556 nucleo-cytoplasmic large DNA viruses in Tara Oceans microbial metagenomes. *ISME J*  
557 2013; **7**: 1678–1695.
- 558 29. Sorensen G, Baker AC, Hall MJ, Munn CB, Schroeder DC. Novel virus dynamics in an  
559 *Emiliana huxleyi* bloom. *Journal of Plankton Research* . 2009. , **31**: 787–791
- 560 30. Wilson WH, Tarran GA, Schroeder D, Cox M, Oke J, Malin G. Isolation of viruses  
561 responsible for the demise of an *Emiliana huxleyi* bloom in the English Channel. *Journal of*  
562 *the Marine Biological Association of the United Kingdom* . 2002. , **82**: 369–377
- 563 31. Lehahn Y, Koren I, Schatz D, Frada M, Sheyn U, Boss E, et al. Decoupling physical from  
564 biological processes to assess the impact of viruses on a mesoscale algal bloom. *Curr Biol*  
565 2014; **24**: 2041–2046.
- 566 32. Tarutani K, Nagasaki K, Yamaguchi M. Viral impacts on total abundance and clonal  
567 composition of the harmful bloom-forming phytoplankton *Heterosigma akashiwo*. *Appl*  
568 *Environ Microbiol* 2000; **66**: 4916–4920.
- 569 33. Sandaa RA, Heldal M, Castberg T, Thyrhaug R, Bratbak G. Isolation and characterization  
570 of two viruses with large genome size infecting *Chrysochromulina ericina*  
571 (Prymnesiophyceae) and *Pyramimonas orientalis* (Prasinophyceae). *Virology* 2001; **290**.
- 572 34. Brussaard CP, Short SM, Frederickson CM, Suttle CA. Isolation and phylogenetic analysis  
573 of novel viruses infecting the phytoplankton *Phaeocystis globosa* (Prymnesiophyceae).  
574 *Appl Environ Microbiol* 2004; **70**.
- 575 35. Kaneko H, Blanc-Mathieu R, Endo H, Chaffron S, Delmont TO, Gaia M, et al. Eukaryotic  
576 virus composition can predict the efficiency of carbon export in the global ocean. *iScience*

- 577 2020; **24**.
- 578 36. Laber CP, Hunter JE, Carvalho F, Collins JR, Hunter EJ, Schieler BM, et al. Coccolithovirus  
579 facilitation of carbon export in the North Atlantic. *Nature microbiology* 2018; **3**.
- 580 37. Kavagutti VS, Bulzu P-A, Chiriac CM, Salcher MM, Mukherjee I, Shabarova T, et al. High-  
581 resolution metagenomic reconstruction of the freshwater spring bloom. *Microbiome* 2023;  
582 **11**: 1–24.
- 583 38. Thurber RV, Haynes M, Breitbart M, Wegley L, Rohwer F. Laboratory procedures to  
584 generate viral metagenomes. *Nat Protoc* 2009; **4**: 470–483.
- 585 39. Schulz F, Roux S, Paez-Espino D, Jungbluth S, Walsh DA, Denev VJ, et al. Giant virus  
586 diversity and host interactions through global metagenomics. *Nature* 2020; **578**: 432–436.
- 587 40. Bäckström D, Yutin N, Jørgensen SL, Dharamshi J, Homa F, Zaremba-Niedwiedzka K, et  
588 al. Virus Genomes from Deep Sea Sediments Expand the Ocean Megavirome and Support  
589 Independent Origins of Viral Gigantism. *MBio* 2019; **10**.
- 590 41. Gaïa M, Meng L, Pelletier E, Forterre P, Vanni C, Fernandez-Guerra A, et al. Plankton-  
591 infecting relatives of herpesviruses clarify the evolutionary trajectory of giant viruses.  
592 *bioRxiv* . 2022. , 2021.12.27.474232
- 593 42. Biller SJ, Berube PM, Dooley K, Williams M, Satinsky BM, Hackl T, et al. Marine microbial  
594 metagenomes sampled across space and time. *Scientific Data* 2018; **5**: 1–7.
- 595 43. Chow C-ET, Suttle CA. Biogeography of Viruses in the Sea. *Annu Rev Virol* 2015; **2**: 41–  
596 66.
- 597 44. Endo H, Ogata H, Suzuki K. Contrasting biogeography and diversity patterns between  
598 diatoms and haptophytes in the central Pacific Ocean. *Sci Rep* 2018; **8**: 1–13.
- 599 45. Sow SLS, Trull TW, Bodrossy L. Oceanographic Fronts Shape Phaeocystis Assemblages:  
600 A High-Resolution 18S rRNA Gene Survey From the Ice-Edge to the Equator of the South  
601 Pacific. *Front Microbiol* 2020; **0**.
- 602 46. Schvarcz CR, Steward GF. A giant virus infecting green algae encodes key fermentation

- 603 genes. *Virology* 2018; **518**: 423–433.
- 604 47. Chelkha N, Lévassieur A, Pontarotti P, Raoult D, Scola BL, Colson P. A Phylogenomic  
605 Study of *Acanthamoeba polyphaga* Draft Genome Sequences Suggests Genetic  
606 Exchanges With Giant Viruses. *Front Microbiol* 2018; **0**.
- 607 48. Fischer MG, Allen MJ, Wilson WH, Suttle CA. Giant virus with a remarkable complement of  
608 genes infects marine zooplankton. *Proc Natl Acad Sci U S A* 2010; **107**: 19508–19513.
- 609 49. Abrahão J, Silva L, Silva LS, Khalil JYB, Rodrigues R, Arantes T, et al. Tailed giant  
610 Tupanvirus possesses the most complete translational apparatus of the known virosphere.  
611 *Nat Commun* 2018; **9**: 1–12.
- 612 50. Meng L, Endo H, Blanc-Mathieu R, Chaffron S, Hernández-Velázquez R, Kaneko H, et al.  
613 Quantitative Assessment of Nucleocytoplasmic Large DNA Virus and Host Interactions  
614 Predicted by Co-occurrence Analyses. *mSphere* 2021; **6**.
- 615 51. Moniruzzaman M, Wurch LL, Alexander H, Dyhrman ST, Gobler CJ, Wilhelm SW. Virus-  
616 host relationships of marine single-celled eukaryotes resolved from metatranscriptomics.  
617 *Nat Commun* 2017; **8**: 16054.
- 618 52. Massana R. Picoeukaryotes. *Encyclopedia of Microbiology (Third Edition)*. 2009. Academic  
619 Press, pp 674–688.
- 620 53. Derelle E, Monier A, Cooke R, Worden AZ, Grimsley NH, Moreau H. Diversity of Viruses  
621 Infecting the Green Microalga *Ostreococcus lucimarinus*. *J Virol* 2015; **89**: 5812–5821.
- 622 54. Bellec L, Grimsley N, Desdevises Y. Isolation of prasinoviruses of the green unicellular  
623 algae *Ostreococcus* spp. on a worldwide geographical scale. *Appl Environ Microbiol* 2010;  
624 **76**: 96–101.
- 625 55. Farzad R, Ha AD, Aylward FO. Diversity and genomics of giant viruses in the North Pacific  
626 Subtropical Gyre. *Front Microbiol* 2022; **13**: 1021923.
- 627 56. Chaudhary C, Saeedi H, Costello MJ. Bimodality of Latitudinal Gradients in Marine Species  
628 Richness. *Trends Ecol Evol* 2016; **31**: 670–676.

- 629 57. Chown SL, Sinclair BJ, Leinaas HP, Gaston KJ. Hemispheric Asymmetries in Biodiversity—  
630 A Serious Matter for Ecology. *PLoS Biol* 2004; **2**: e406.
- 631 58. Ibarbalz FM, Henry N, Brandão MC, Martini S, Busseni G, Byrne H, Coelho LP, Endo H,  
632 Gasol JM, Gregory AC, Mahé F, Rigonato J, Royo-Llonch M, Salazar G, Sanz-Sáez I,  
633 Scalco E, Soviadan D, Zayed AA, Zingone A, Labadie K, Ferland J, Marec C, Kandels S,  
634 Picheral M, Dimier C, Poulain J, Pisarev S, Carmichael M, Pesant S}, de Vargas C Karp-  
635 Boss L Wincker P Lombard F Bowler C Zinger L Tara Oceans Coordinators Babin M Boss  
636 E Iudicone D Jaillon O Acinas Sg Ogata H Pelletier E Stemmann L Sullivan Mb Sunagawa  
637 S Bopp L. Global Trends in Marine Plankton Diversity across Kingdoms of Life. *Cell* 2019;  
638 **179**: 1084–1097.e21.
- 639 59. Hillebrand H. Strength, slope and variability of marine latitudinal gradients. *Marine Ecology*  
640 *Progress Series* . 2004. , **273**: 251–267
- 641 60. Tittensor DP, Mora C, Jetz W, Lotze HK, Ricard D, Berghe EV, et al. Global patterns and  
642 predictors of marine biodiversity across taxa. *Nature* 2010; **466**: 1098–1101.
- 643 61. Chen I-C, Hill JK, Ohlemüller R, Roy DB, Thomas CD. Rapid range shifts of species  
644 associated with high levels of climate warming. *Science* 2011; **333**: 1024–1026.
- 645 62. Poloczanska ES, Brown CJ, Sydeman WJ, Kiessling W, Schoeman DS, Moore PJ, et al.  
646 Global imprint of climate change on marine life. *Nat Clim Chang* 2013; **3**: 919–925.
- 647 63. Pinsky ML, Worm B, Fogarty MJ, Sarmiento JL, Levin SA. Marine taxa track local climate  
648 velocities. *Science* 2013; **341**: 1239–1242.
- 649 64. García Molinos J, Halpern BS, Schoeman DS, Brown CJ, Kiessling W, Moore PJ, et al.  
650 Climate velocity and the future global redistribution of marine biodiversity. *Nat Clim Chang*  
651 2015; **6**: 83–88.
- 652 65. Li T, Philander SGH. On the Seasonal Cycle of the Equatorial Atlantic Ocean. *J Clim* 1997;  
653 **10**: 813–817.
- 654 66. Longhurst AR. *Ecological Geography of the Sea*. 2010. Elsevier.

- 655 67. Santini S, Jeudy S, Bartoli J, Poirot O, Lescot M, Abergel C, et al. Genome of Phaeocystis  
656 globosa virus PgV-16T highlights the common ancestry of the largest known DNA viruses  
657 infecting eukaryotes. *Proc Natl Acad Sci U S A* 2013; **110**.
- 658 68. Gallot-Lavallée L, Blanc G, Claverie JM. Comparative Genomics of Chrysochromulina  
659 Ericina Virus and Other Microalga-Infecting Large DNA Viruses Highlights Their Intricate  
660 Evolutionary Relationship with the Established Mimiviridae Family. *J Virol* 2017; **91**.
- 661 69. Stough JMA, Yutin N, Chaban YV, Moniruzzaman M, Gann ER, Pound HL, et al. Genome  
662 and Environmental Activity of a Chrysochromulina parva Virus and Its Virophages. *Front*  
663 *Microbiol* 2019; **10**.
- 664 70. Yutin N, Koonin EV. Hidden evolutionary complexity of Nucleo-Cytoplasmic Large DNA  
665 viruses of eukaryotes. *Virology* 2012; **9**: 1–18.
- 666 71. Raoult D, Audic S, Robert C, Abergel C, Renesto P, Ogata H, et al. The 1.2-megabase  
667 genome sequence of Mimivirus. *Science* 2004; **306**.
- 668 72. Saini HK, Fischer D. Structural and functional insights into Mimivirus ORFans. *BMC*  
669 *Genomics* 2007; **8**.
- 670 73. Abrahão JS, Araújo R, Colson P, La Scola B. The analysis of translation-related gene set  
671 boosts debates around origin and evolution of mimiviruses. *PLoS Genet* 2017; **13**:  
672 e1006532.
- 673 74. Silva LCF, Almeida GMF, Assis FL, Albarnaz JD, Boratto PVM, Dornas FP, et al.  
674 Modulation of the expression of mimivirus-encoded translation-related genes in response to  
675 nutrient availability during *Acanthamoeba castellanii* infection. *Front Microbiol* 2015; **0**.
- 676 75. Behrenfeld MJ, Kolber ZS. Widespread iron limitation of phytoplankton in the south pacific  
677 ocean. *Science* 1999; **283**: 840–843.
- 678 76. Revilla Y, Cebrián A, Baixeras E, Martínez C, Viñuela E, Salas ML. Inhibition of apoptosis  
679 by the African swine fever virus Bcl-2 homologue: role of the BH1 domain. *Virology* 1997;  
680 **228**.

- 681 77. Bidle KD, Kwityn CJ. Assessing The Role Of Caspase Activity And Metacaspase  
682 Expression On Viral Susceptibility Of The Coccolithophore, *Emiliana Huxleyi* (Haptophyta).  
683 *J Phycol* 2012; **48**: 1079–1089.
- 684 78. Du J, Wang L, Wang Y, Shen J, Pan C, Meng Y, et al. Autophagy and apoptosis induced  
685 by Chinese giant salamander (*Andrias davidianus*) iridovirus (CGSIV). *Vet Microbiol* 2016;  
686 **195**: 87–95.
- 687 79. Schrad JR, Abrahão JS, Cortines JR, Parent KN. Structural and Proteomic Characterization  
688 of the Initiation of Giant Virus Infection. *Cell* 2020; **181**: 1046–1061.e6.
- 689 80. Lartigue A, Burlat B, Coutard B, Chaspoul F, Claverie J-M, Abergel C. The megavirus  
690 chilensis Cu,Zn-superoxide dismutase: the first viral structure of a typical cellular copper  
691 chaperone-independent hyperstable dimeric enzyme. *J Virol* 2015; **89**: 824–832.
- 692 81. Van Etten JL, Meints RH. Giant viruses infecting algae. *Annu Rev Microbiol* 1999; **53**: 447–  
693 494.
- 694 82. Furuta M, Schrader JO, Schrader HS, Kokjohn TA, Nyaga S, McCullough AK, et al.  
695 *Chlorella* virus PBCV-1 encodes a homolog of the bacteriophage T4 UV damage repair  
696 gene denV. *Appl Environ Microbiol* 1997; **63**: 1551–1556.
- 697 83. Redrejo-Rodríguez M, Ishchenko A, Saparbaev MK, Salas ML, Salas J. African swine fever  
698 virus AP endonuclease is a redox-sensitive enzyme that repairs alkylating and oxidative  
699 damage to DNA. *Virology* 2009; **390**: 102–109.
- 700 84. Manandhar M, Boulware KS, Wood RD. The ERCC1 and ERCC4 (XPF) genes and gene  
701 products. *Gene* 2015; **569**: 153.
- 702 85. Wilson WH, Gilg IC, Duarte A, Ogata H. Development of DNA mismatch repair gene, MutS,  
703 as a diagnostic marker for detection and phylogenetic analysis of algal Megaviruses.  
704 *Virology* 2014; **466-467**: 123–128.
- 705 86. Ogata H, Ray J, Toyoda K, Sandaa R-A, Nagasaki K, Bratbak G, et al. Two new  
706 subfamilies of DNA mismatch repair proteins (MutS) specifically abundant in the marine

- 707 environment. *ISME J* 2011; **5**: 1143–1151.
- 708 87. Piacente F, De Castro C, Jeudy S, Molinaro A, Salis A, Damonte G, et al. Giant Virus  
709 Megavirus chilensis Encodes the Biosynthetic Pathway for Uncommon Acetamido Sugars.  
710 *J Biol Chem* 2014; **289**: 24428–24439.
- 711 88. Parakkottil Chothi M, Duncan GA, Armirotti A, Abergel C, Gurnon JR, Van Etten JL, et al.  
712 Identification of an L-rhamnose synthetic pathway in two nucleocytoplasmic large DNA  
713 viruses. *J Virol* 2010; **84**: 8829–8838.
- 714 89. Rodrigues RAL, dos Santos Silva LK, Dornas FP, de Oliveira DB, Magalhães TFF, Santos  
715 DA, et al. Mimivirus Fibrils Are Important for Viral Attachment to the Microbial World by a  
716 Diverse Glycoside Interaction Repertoire. *J Virol* 2015; **89**: 11812.
- 717 90. Geslin C, Gaillard M, Flament D, Rouault K, Le Romancer M, Prieur D, et al. Analysis of the  
718 first genome of a hyperthermophilic marine virus-like particle, PAV1, isolated from  
719 *Pyrococcus abyssi*. *J Bacteriol* 2007; **189**: 4510–4519.
- 720 91. Rose SL, Fulton JM, Brown CM, Natale F, Van Mooy BAS, Bidle KD. Isolation and  
721 characterization of lipid rafts in *Emiliana huxleyi*: a role for membrane microdomains in  
722 host-virus interactions. *Environ Microbiol* 2014; **16**: 1150–1166.
- 723 92. Aylward FO, Moniruzzaman M. ViralRecall-A Flexible Command-Line Tool for the Detection  
724 of Giant Virus Signatures in 'Omic Data. *Viruses* 2021; **13**.
- 725 93. Olm MR, Brown CT, Brooks B, Banfield JF. dRep: a tool for fast and accurate genomic  
726 comparisons that enables improved genome recovery from metagenomes through de-  
727 replication. *ISME J* 2017; **11**: 2864–2868.
- 728 94. Weinheimer AR, Aylward FO. Infection strategy and biogeography distinguish cosmopolitan  
729 groups of marine jumbo bacteriophages. *ISME J* 2022; **16**: 1657–1667.
- 730 95. Capella-Gutiérrez S, Silla-Martínez JM, Gabaldón T. trimAl: a tool for automated alignment  
731 trimming in large-scale phylogenetic analyses. *Bioinformatics* 2009; **25**: 1972–1973.
- 732 96. Minh BQ, Schmidt HA, Chernomor O, Schrempf D, Woodhams MD, von Haeseler A, et al.

- 733 IQ-TREE 2: New Models and Efficient Methods for Phylogenetic Inference in the Genomic  
734 Era. *Mol Biol Evol* 2020; **37**: 1530–1534.
- 735 97. Lemos LN, Fulthorpe RR, Triplett EW, Roesch LFW. Rethinking microbial diversity analysis  
736 in the high throughput sequencing era. *J Microbiol Methods* 2011; **86**: 42–51.
- 737 98. Schlitzer R. Data Analysis and Visualization with Ocean Data View.  
738 [http://dx.doi.org/10.1016/s0098-3004\(02\)00040-7](http://dx.doi.org/10.1016/s0098-3004(02)00040-7) .
- 739 99. Huerta-Cepas J, Szklarczyk D, Heller D, Hernández-Plaza A, Forslund SK, Cook H, et al.  
740 eggNOG 5.0: a hierarchical, functionally and phylogenetically annotated orthology resource  
741 based on 5090 organisms and 2502 viruses. *Nucleic Acids Res* 2018; **47**: D309–D314.
- 742 100. Mistry J, Chuguransky S, Williams L, Qureshi M, Salazar GA, Sonnhammer ELL, et al.  
743 Pfam: The protein families database in 2021. *Nucleic Acids Res* 2020; **49**: D412–D419.
- 744

745 **Figure legends**

746 **Figure 1.** Global map of sampling locations, colored by transect. Blue dots indicate the start of  
747 cruise tracks.

748 **Figure 2.** Summary of the taxonomy of detected giant viruses. The area of each rectangle is  
749 proportional to the number of identified viral genomes in the respective taxon.

750 **Figure 3.** Unique genomes and genomes shared between the transects (A) and water depth  
751 layers (B). Horizontal bars (right) indicate the total number of genomes found in each transect;  
752 black dots indicate the presence in one or multiple transects; the corresponding vertical bars  
753 indicate the number of genomes with the presence described by the dots.

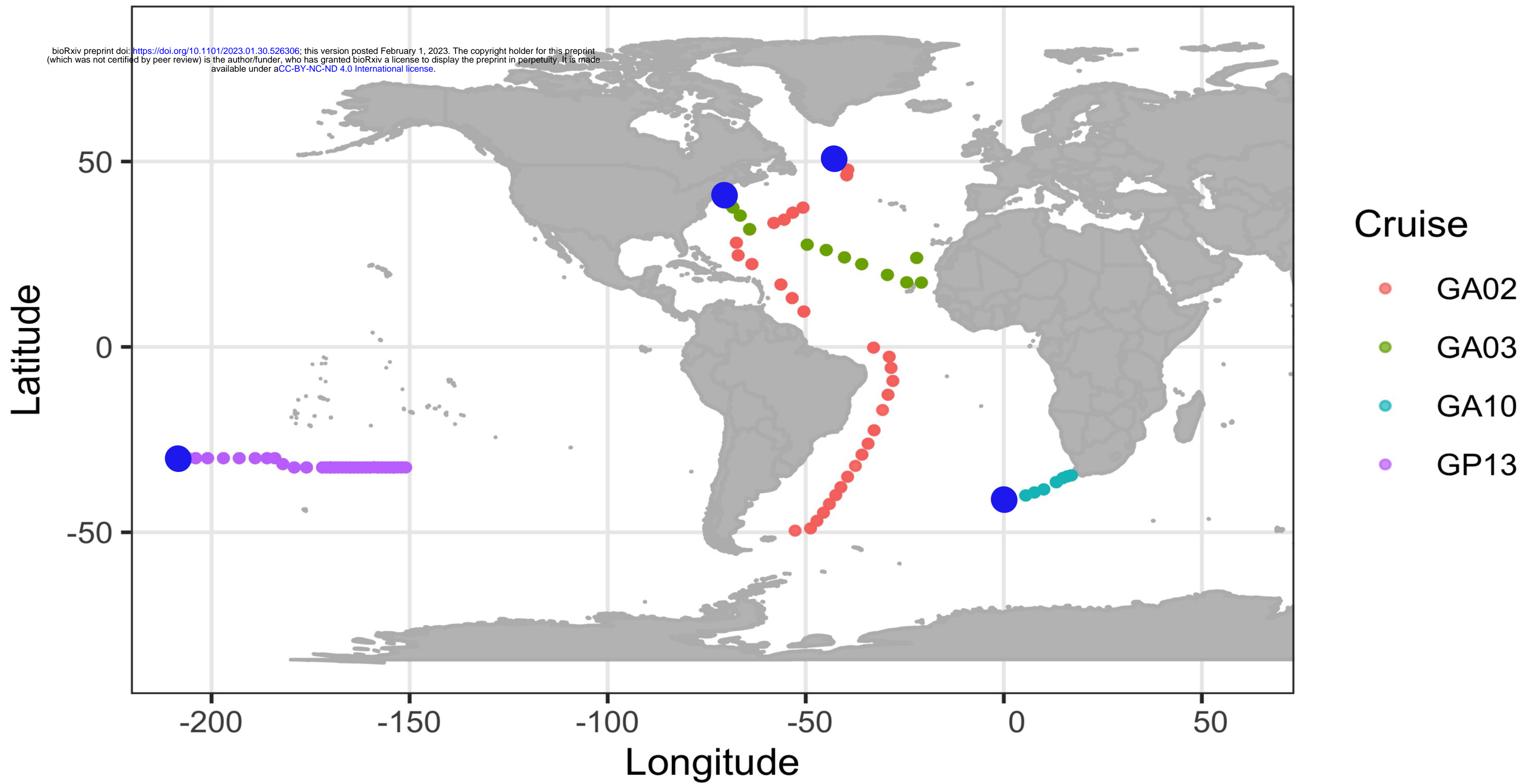
754 **Figure 4.** Distribution of giant viruses in each transect. Each column represents a sampling  
755 location. The y-axis shows the number of different viral genomes that were recovered at a given  
756 location, separated into three depth ranges (2-80m, 80-150m, and 150-5,500m). Locations are  
757 arranged in increasing distance from left to right on the x-axis, based on their distance from the  
758 starting location and follow the indicated orientation (N to S for GA02 and GA03, W to E for  
759 GA10 and GP13).

760 **Figure 5.** Distribution of viruses throughout the water column along the transects. The viral  
761 abundance (calculated in log RPKM) of (A) total giant viruses present in the transect (B) viruses  
762 of the *Imitervirales* order (C) viruses of the *Algavirales* order only. Samples were ordered based  
763 on the distance along transects, beginning from the first sampling location of cruise tracks (0  
764 km). Black dots denote the sampling location along the transect of each sample.

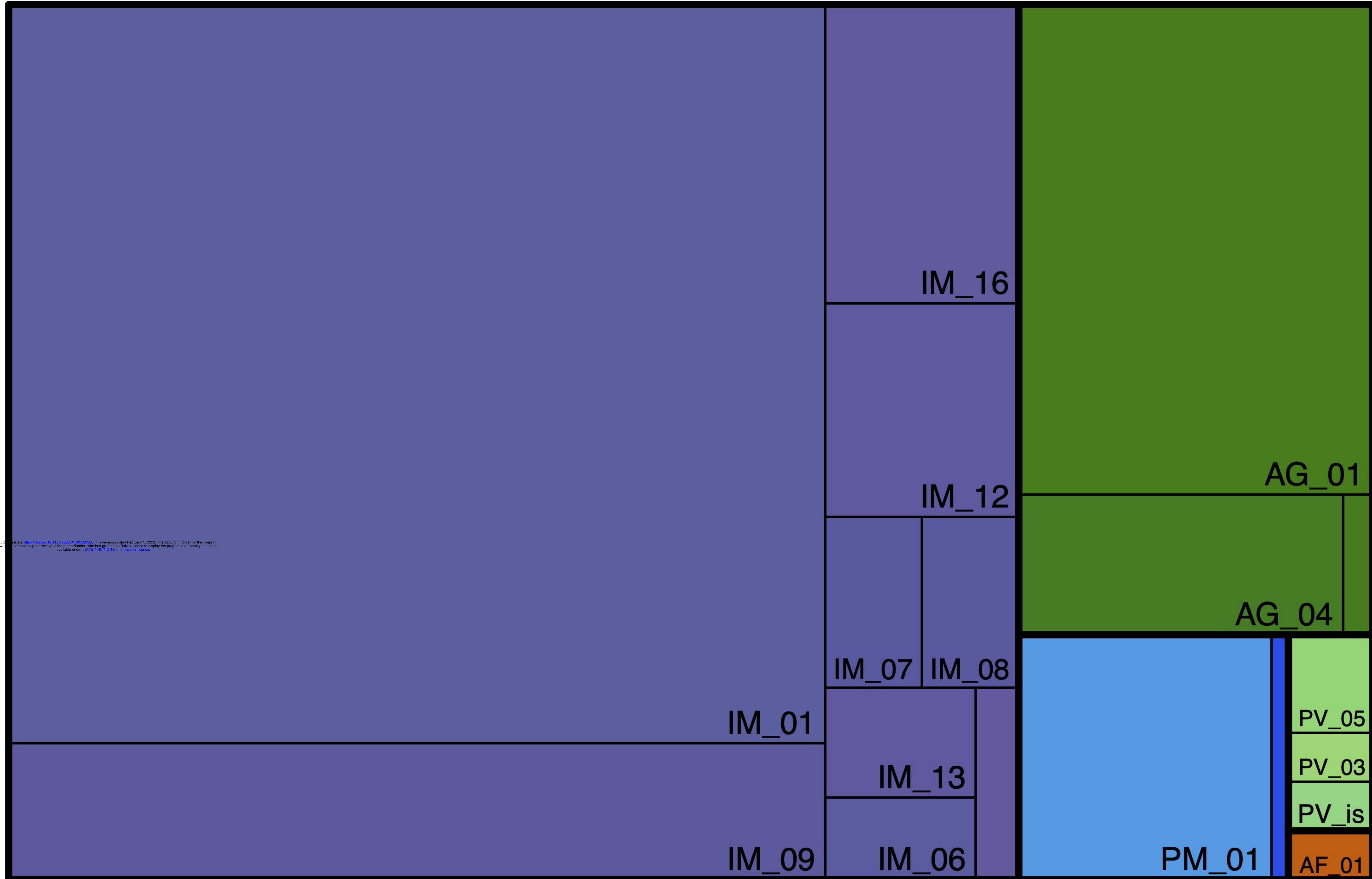
765 **Figure 6.** Latitudinal pattern of giant virus diversity across the transect GA02 showed in (A)  
766 Shannon's H index (B) Genome richness. Stars showing significant difference between two  
767 latitudinal groups (Wilcox test, p-values < 0.05) (\* < 0.05, \*\* < 0.01, \*\*\* < 0.001, \*\*\*\* < 0.0001)  
768 Panels left: Total virus community; center: *Imitervirales* communities; right: *Algavirales*  
769 communities. EQ, Equator.

770 **Figure 7.** Community composition between latitudinal locations NMDS ordination based on  
771 Bray-Curtis distance matrices of viral communities collected in the (A) GA02 transect, stress =  
772 0.3 (B) All four bioGEOTRACES, stress = 0.21. Latitudinal groups are color-coded by sample  
773 locations at higher than 40°N/S, from 20° to 40°N/S, and below 20°N/S (equatorial). Ellipses  
774 represent 95% confidence intervals. Viral communities are significantly different between groups  
775 (Permanova  $p < 0.001$ ).

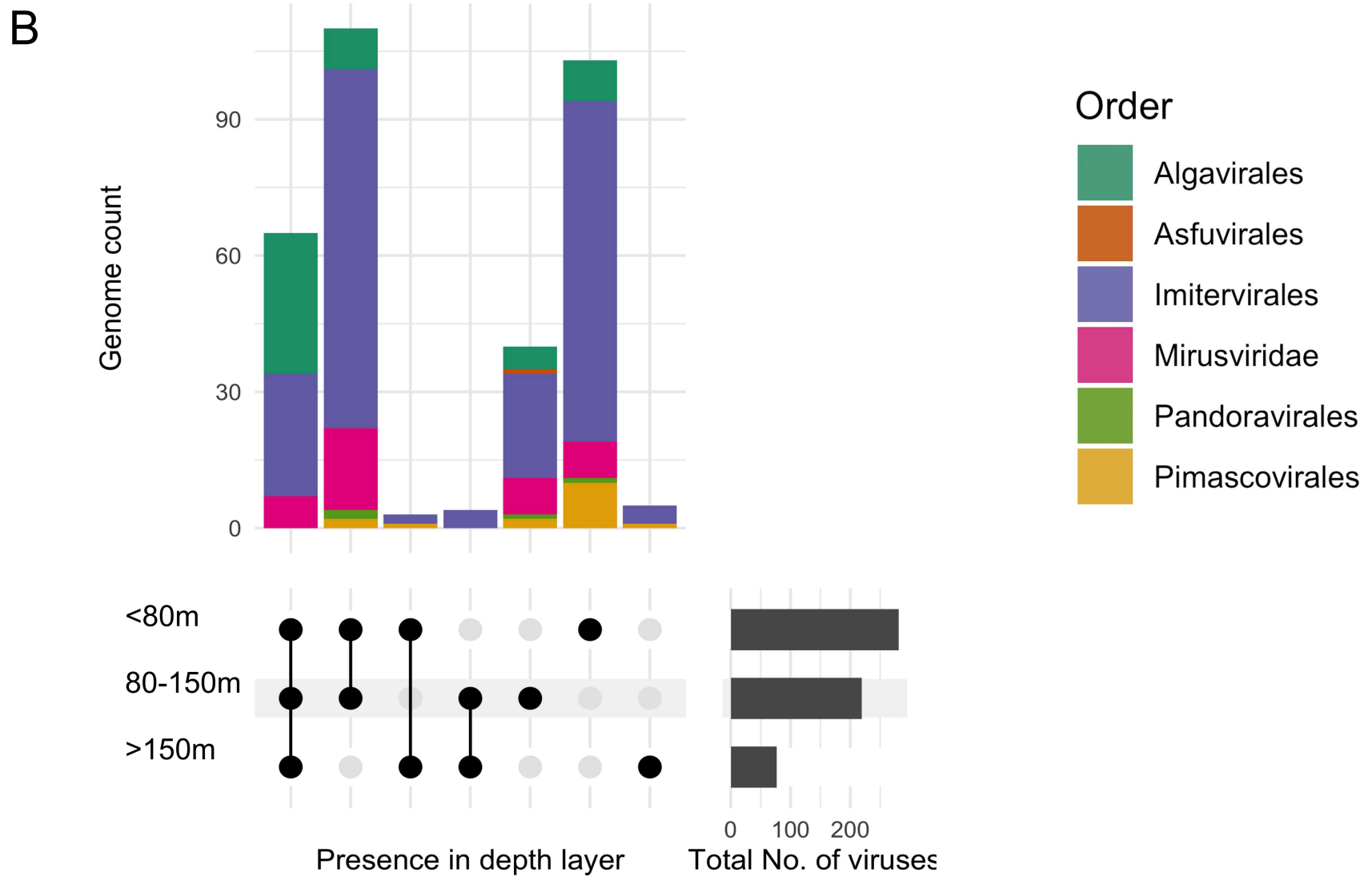
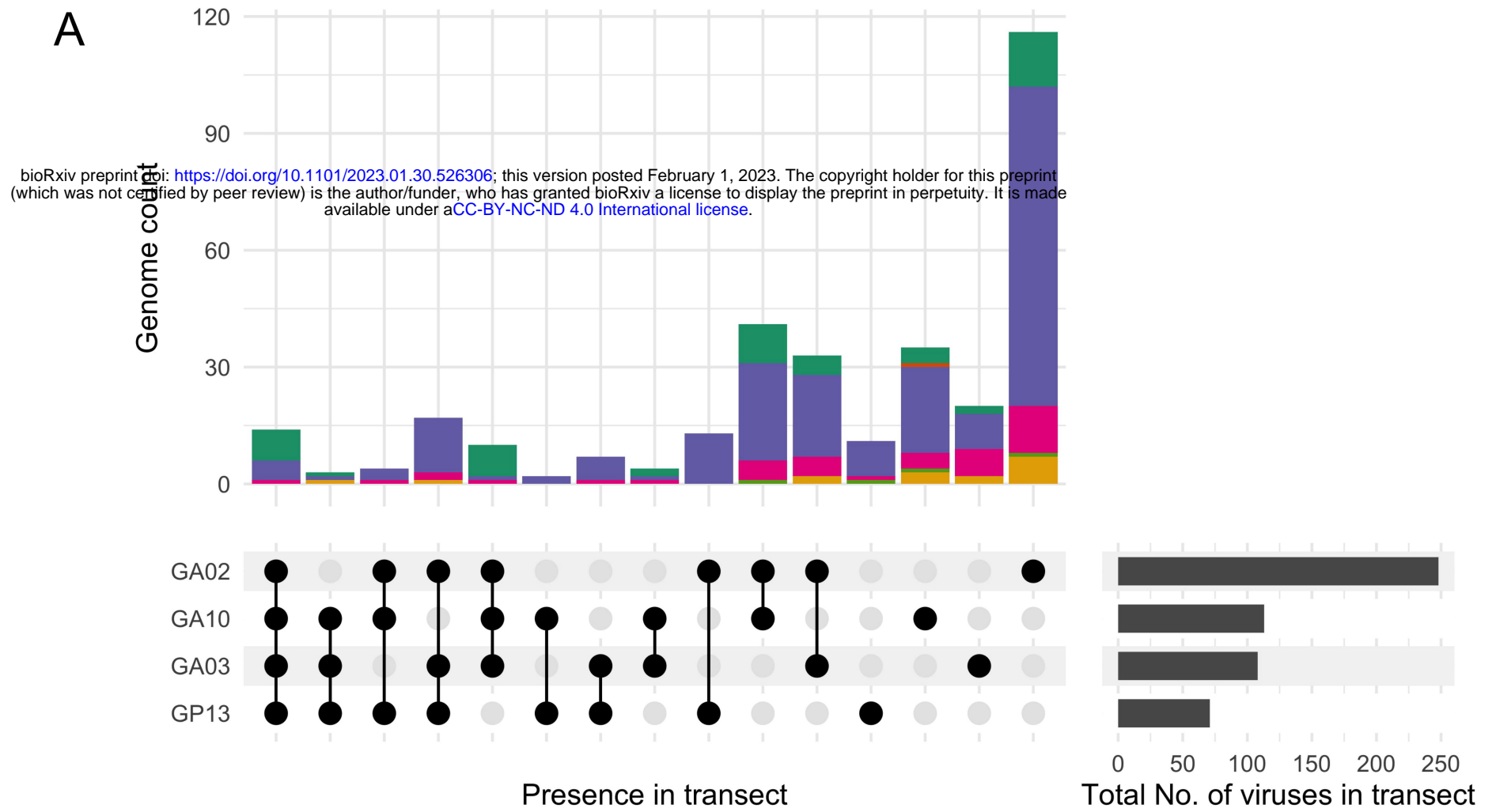
776 **Figure 8.** (A) General mapping statistics of viruses found in surface waters <150m. The y-axis  
777 shows the average abundance of a given individual genome (in RPKM), the x-axis shows the  
778 number of samples from which the virus was recovered. Dots are colored by the viral order and  
779 dot sizes represent the length of the genomes. (B) Genomic functional features of the six  
780 genomes that are widespread in oligotrophic waters. On the x axis, genomes are ranked from  
781 left to right in order of decreasing number of samples in which the viruses were detected; the  
782 horizontal colored bar shows the taxonomic order of the genome (purple: *Imitervirales*, green:  
783 *Algavirales*). The y axis denotes the functional annotation found in genomes; putative genes are  
784 color-coded by functional categories. Gene function abbreviations: PPDK, Pyruvate phosphate  
785 dikinase; GAPDH, Glyceraldehyde 3-P dehydrogenase; SDH, Succinate dehydrogenase;  
786 LHCB, Chlorophyll a/b binding protein; ACAD, Acyl-CoA dehydrogenase; ACBP, Acyl-CoA  
787 binding protein; GMD, GDP-mannose dehydrogenase; GMDH, GDP-mannose 4,6 dehydratase;  
788 GlcNAc epimerase, UDP-N-acetylglucosamine 2-epimerase; GNAT, Glucosamine-6-phosphate  
789 N-acetyltransferase; PCNA, Proliferating cell nuclear antigen; PI3K, Phosphatidylinositol 3-  
790 kinases; PDXK, PD-(D/E)XK nuclease superfamily; TNFR, Tumor necrosis factor receptor.  
791

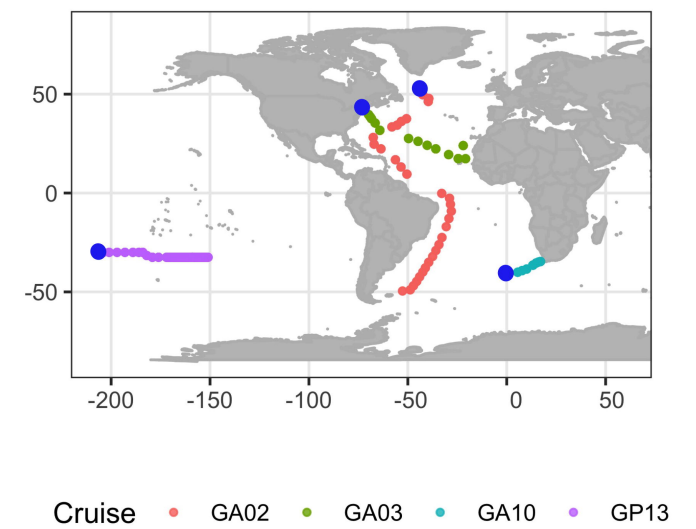
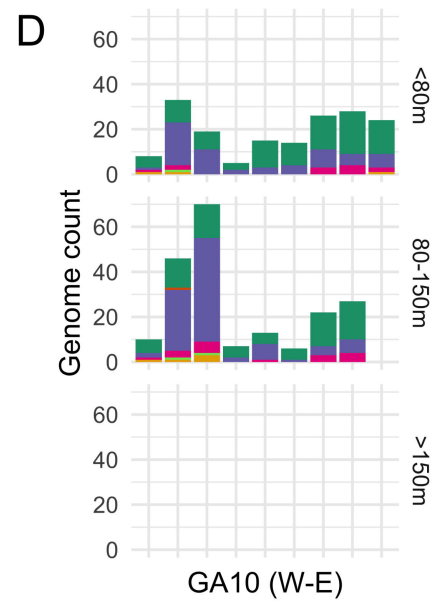
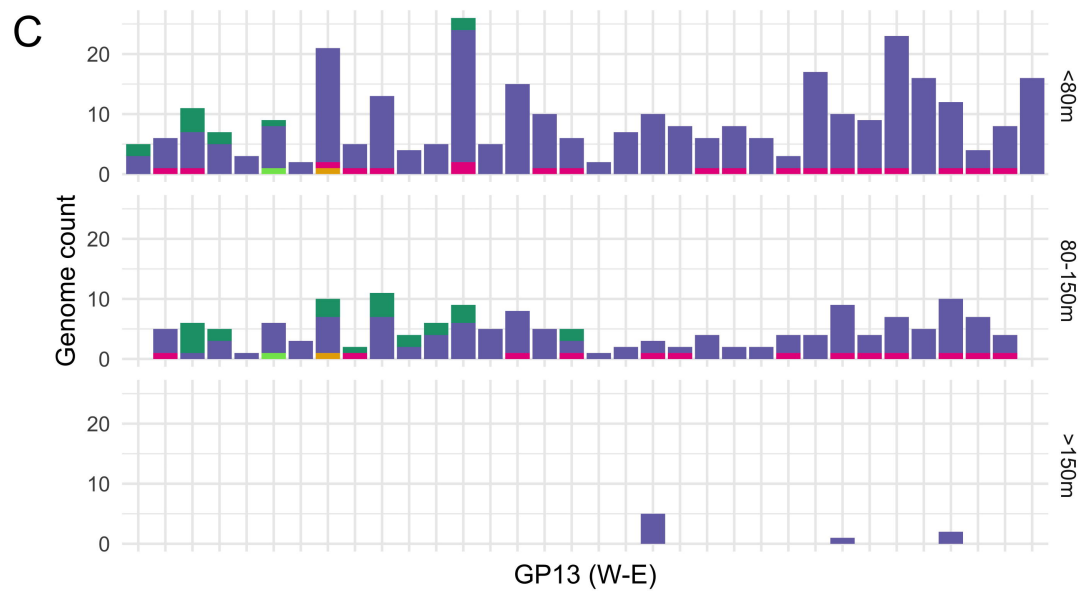
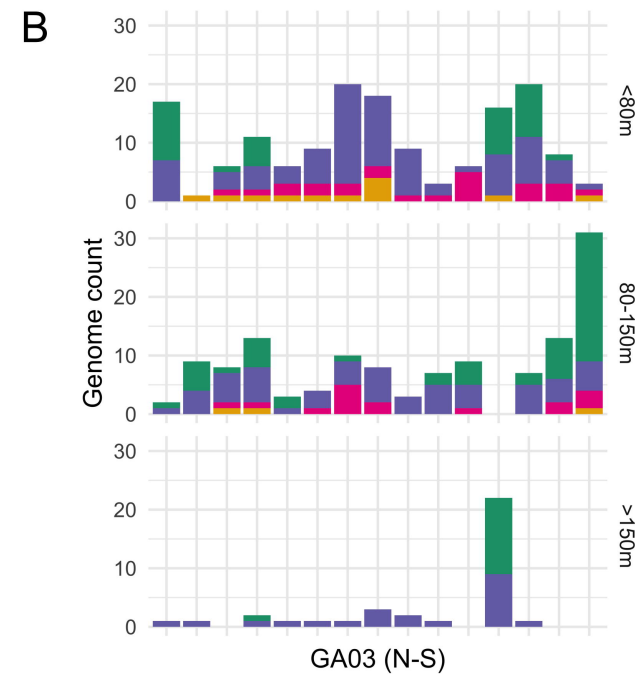
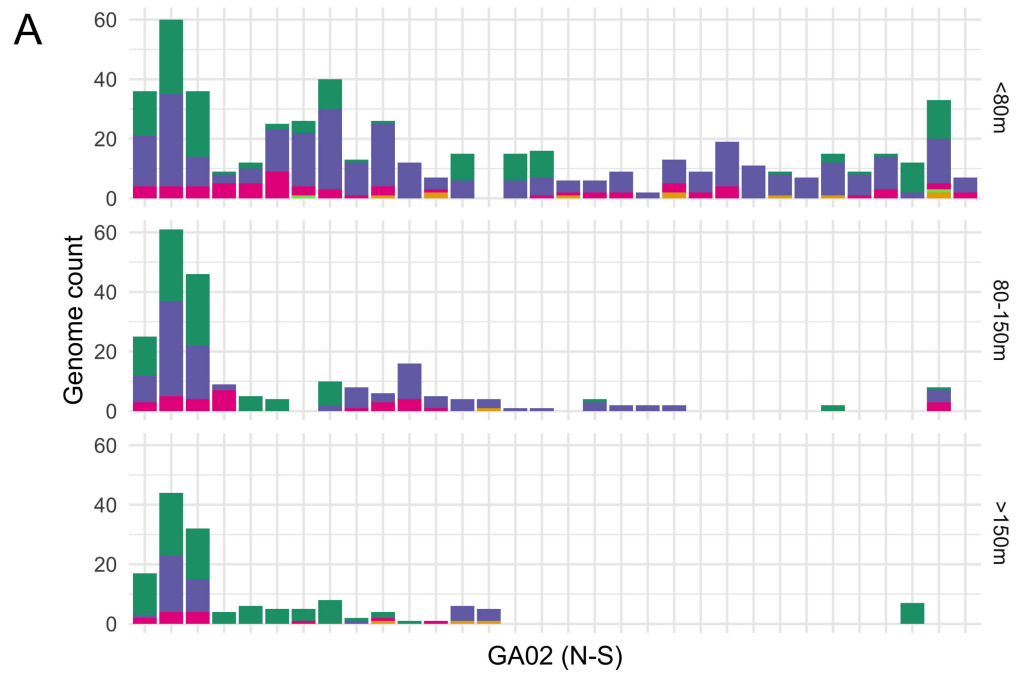


- Algavirales
- Asfuvirales
- Imitervirales
- Pandoravirales
- Pimascovirales

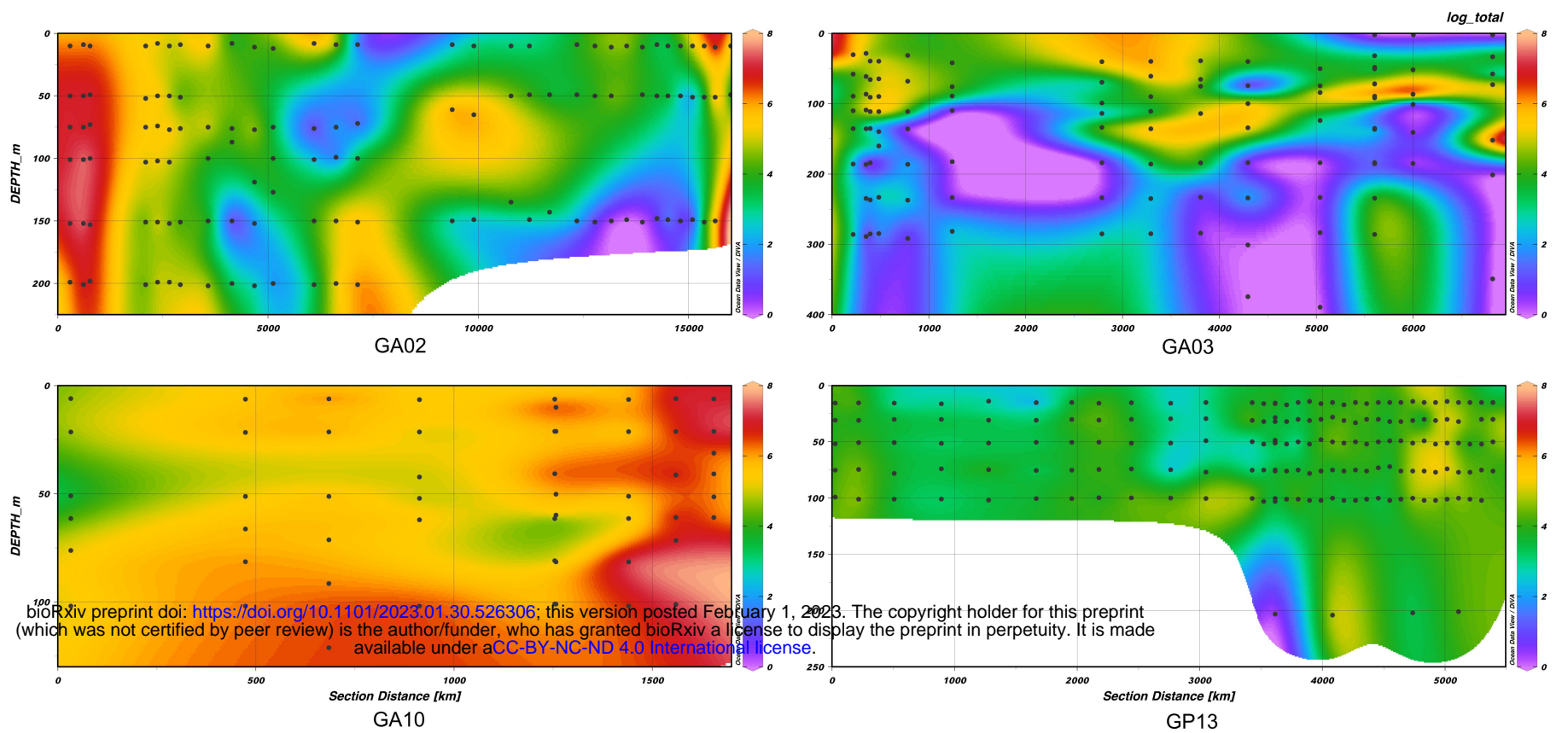


bioRxiv preprint doi: <https://doi.org/10.1101/2023.01.26.526300>; this version posted February 1, 2023. The copyright holder for this preprint (which was not certified by peer review) is the author/funder, who has granted bioRxiv a license to display the preprint in perpetuity. It is made available under aCC-BY-NC-ND 4.0 International license.



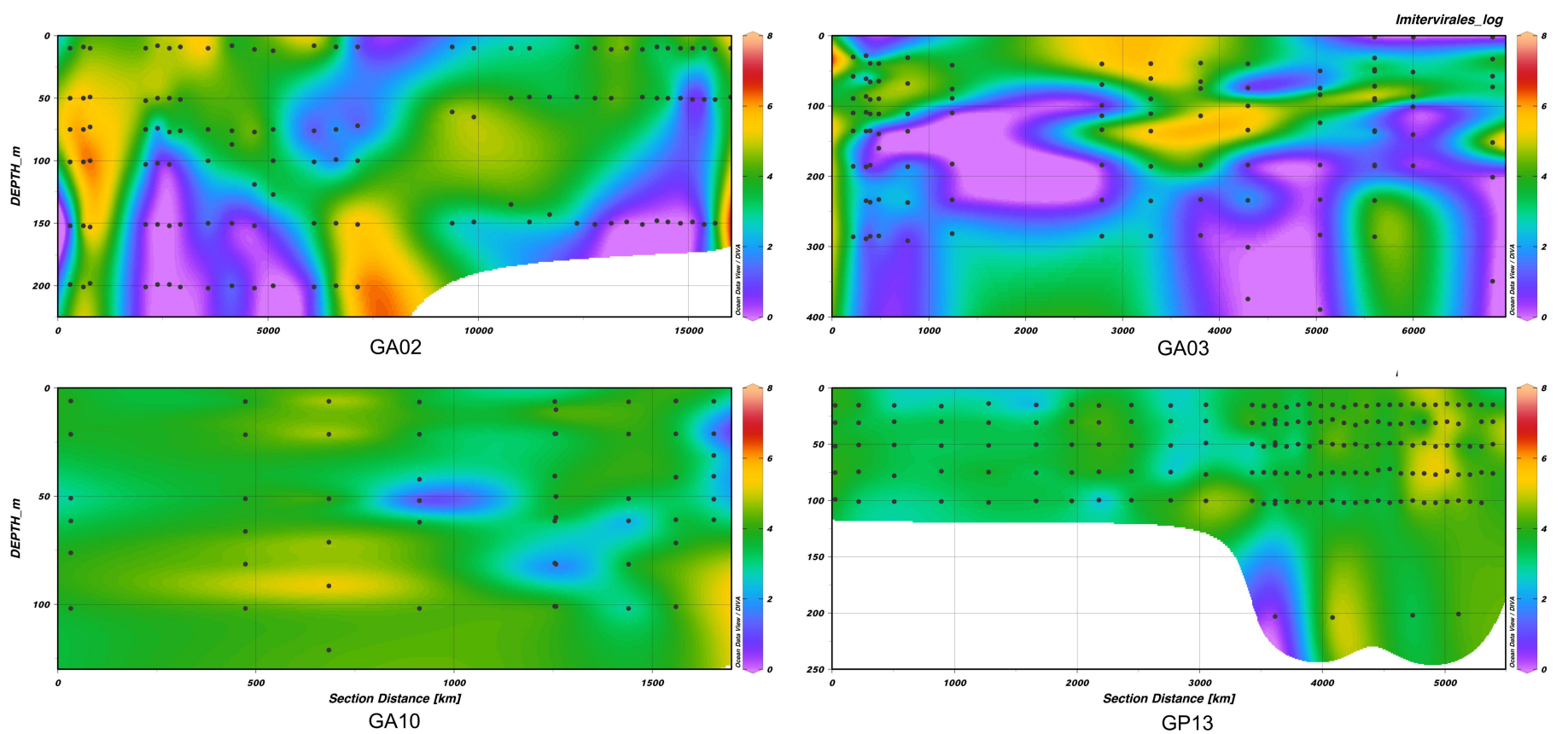


A

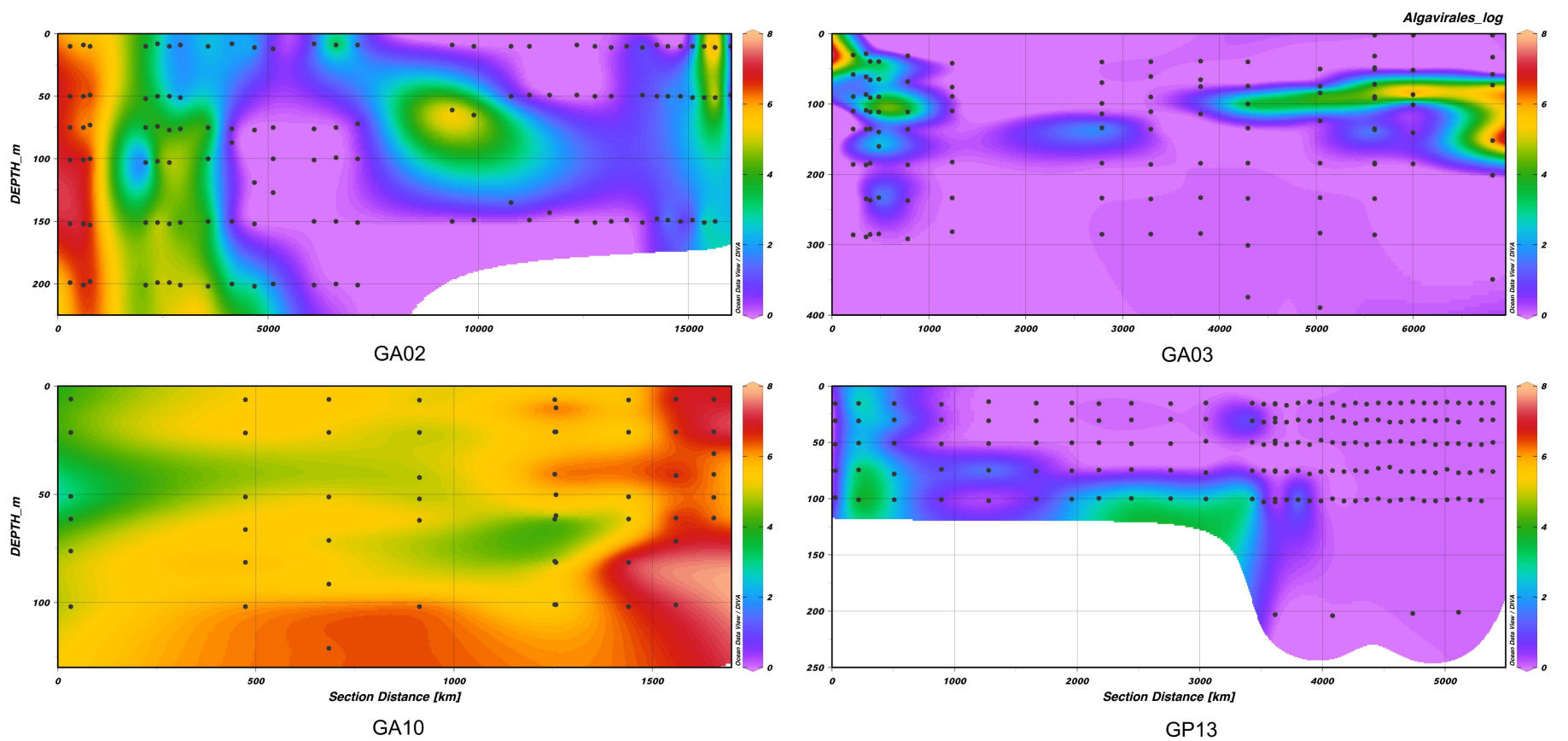


bioRxiv preprint doi: <https://doi.org/10.1101/2023.01.30.526306>; this version posted February 1, 2023. The copyright holder for this preprint (which was not certified by peer review) is the author/funder, who has granted bioRxiv a license to display the preprint in perpetuity. It is made available under aCC-BY-NC-ND 4.0 International license.

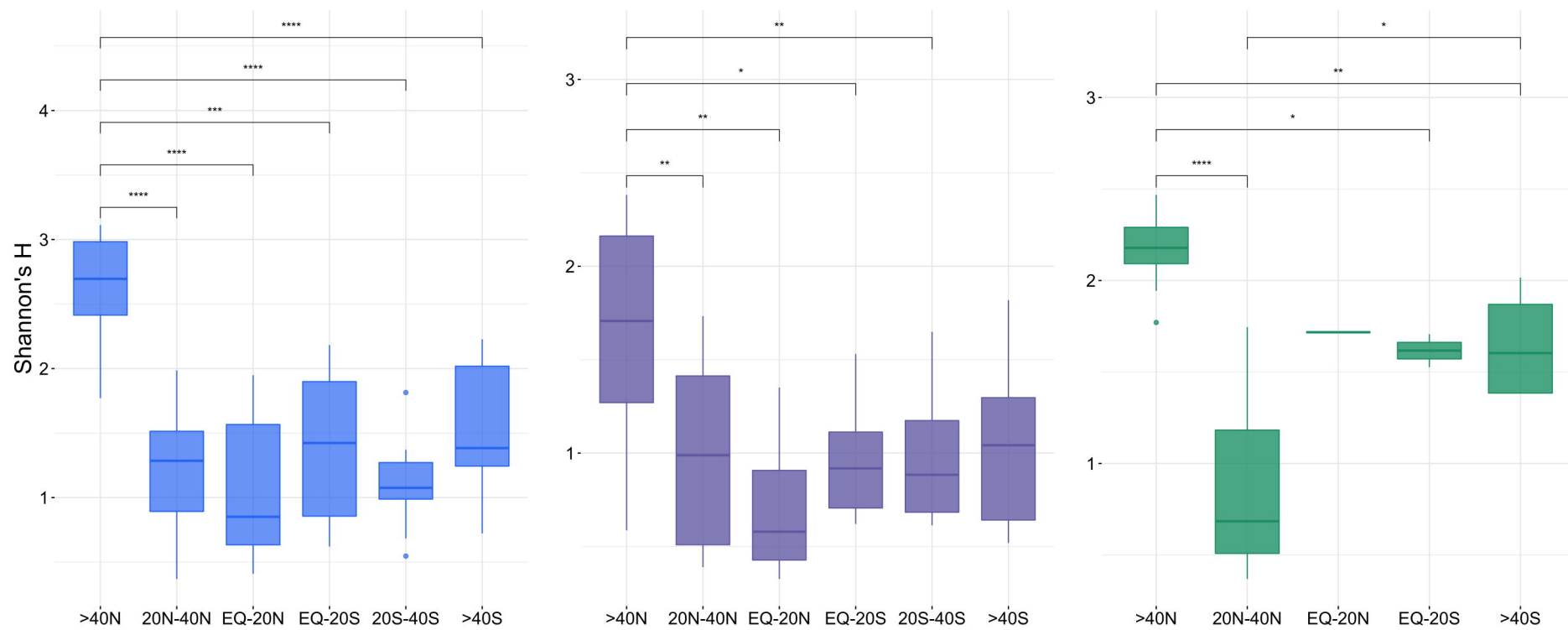
B



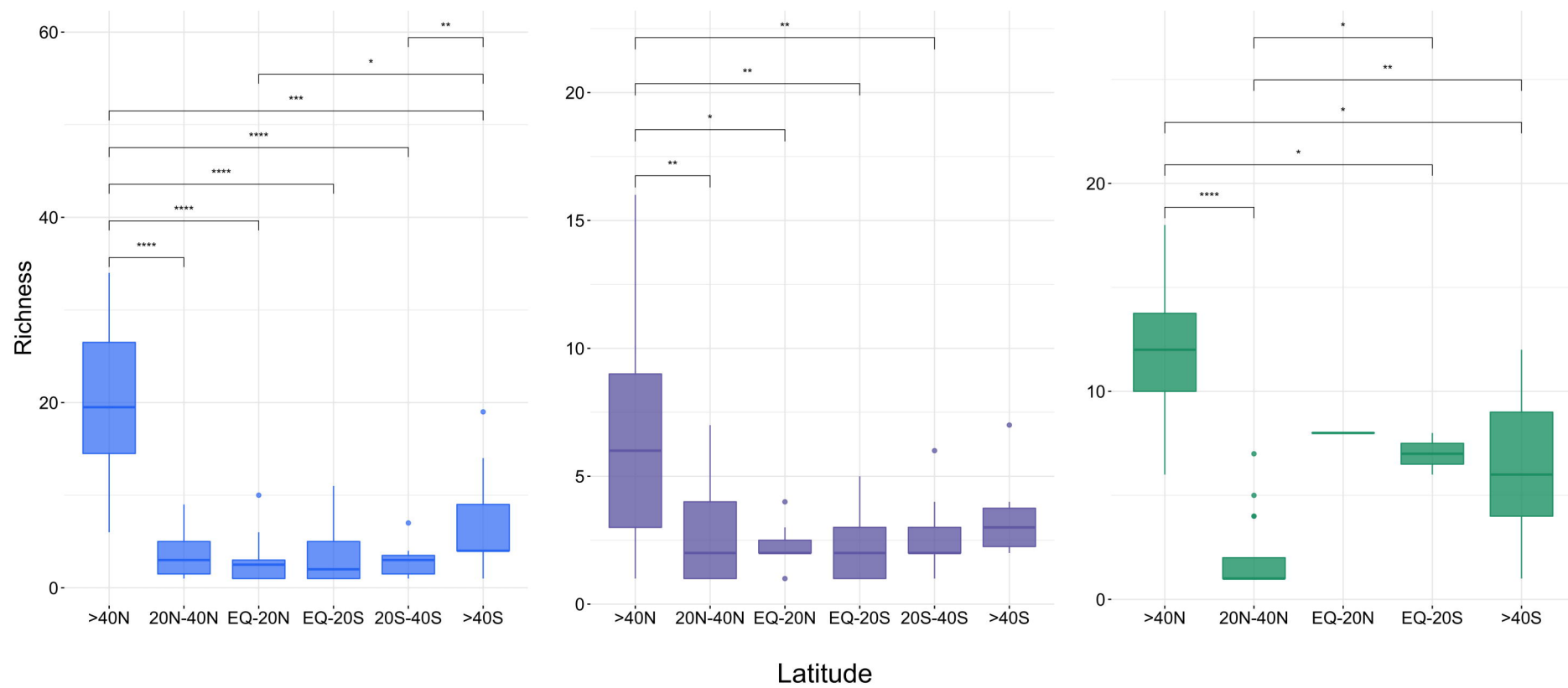
C

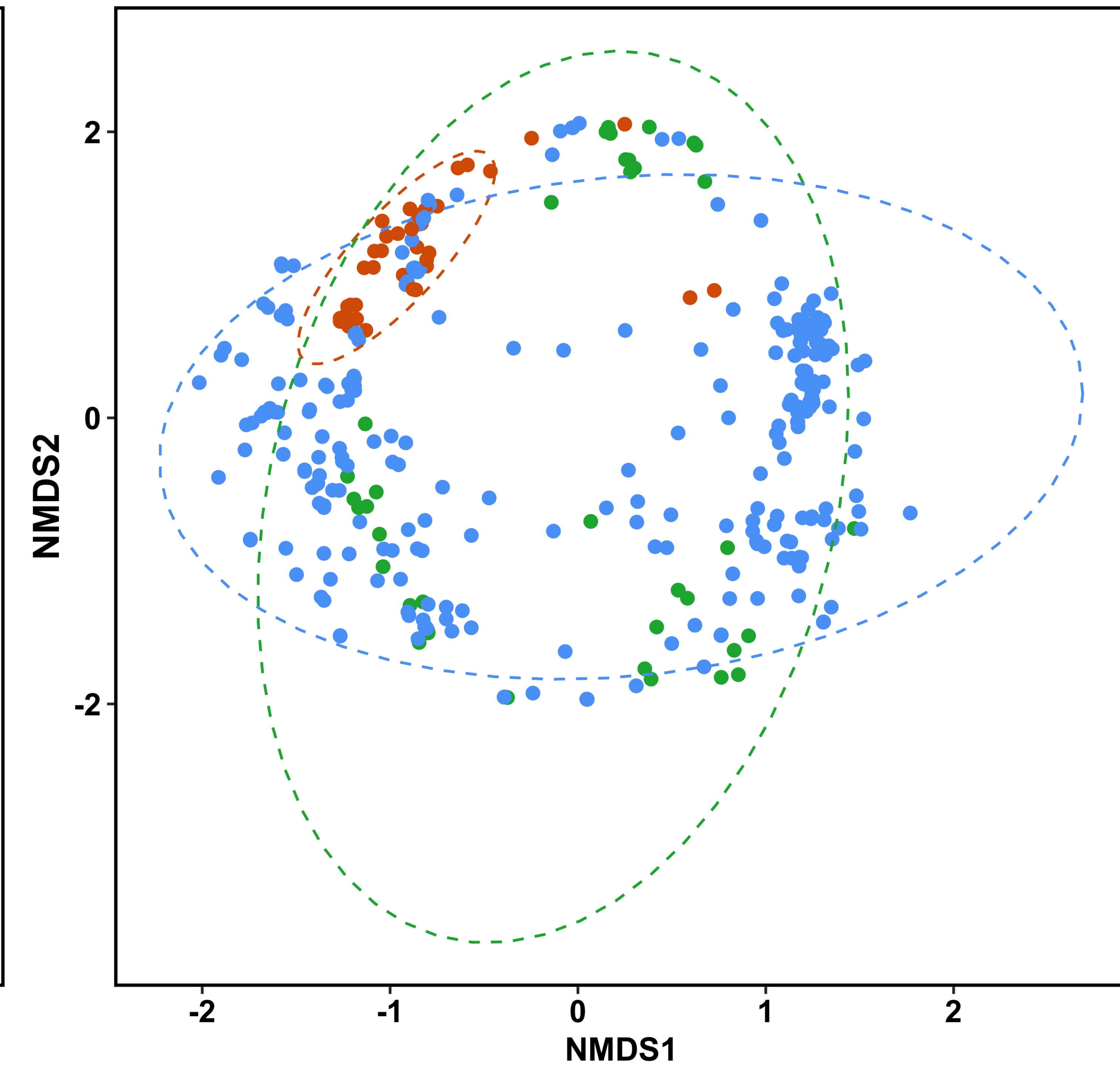
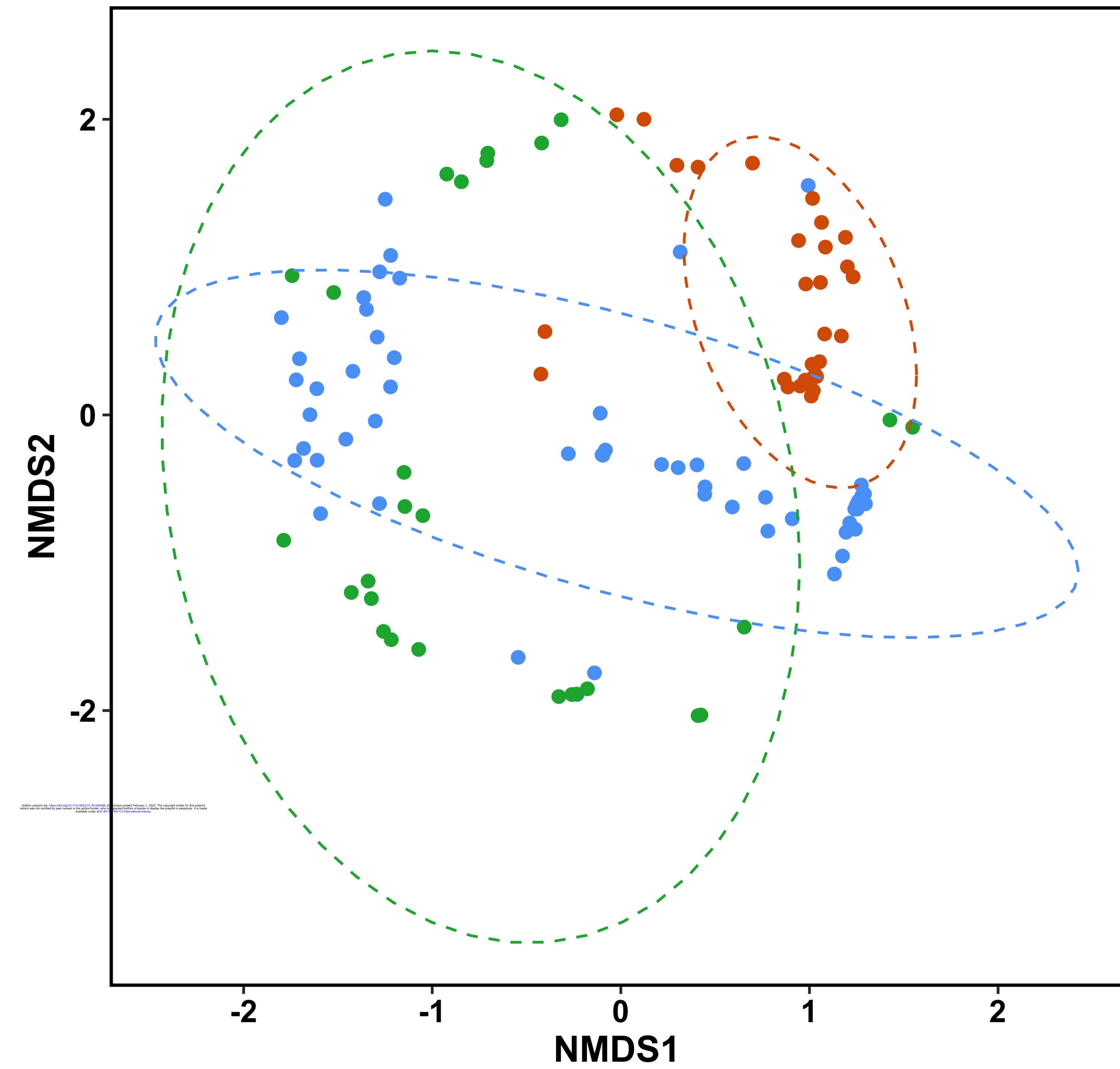


A



B

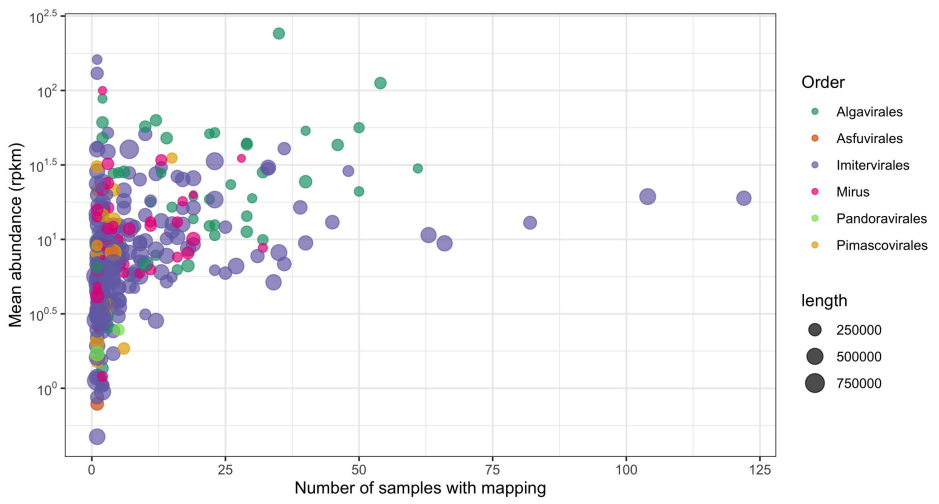




**Latitude**

- high latitudes (><math>40^\circ\text{N/S}</math>)
- low latitudes (<<math>20^\circ\text{N/S}</math>)
- mid latitudes (<math>20\text{-}40^\circ\text{N/S}</math>)

A



B

